New Journal of Physics
An Institute of Physics and Deutsche Physikalische Gesellschaft Journal

Solitons, shocks and vortices in dusty plasmas

P K Shukla and A A Mamun[1]
Institut für Theoretische Physik IV, Fakultät für Physik und Astronomie, Ruhr-Universität Bochum, D-44780 Bochum, Germany
E-mail: ps@tp4.ruhr-uni-bochum.de

New Journal of Physics **5** (2003) 17.1–17.37 (http://www.njp.org/)
Received 4 December 2002
Published 14 March 2003

Abstract. Three important classes of nonlinear phenomena, namely solitons, shocks and vortices in dusty plasmas, have been discussed. The static and mobile charged dust grains have been considered in order to study all of these nonlinear phenomena. The effects of nonplanar geometry, dust grain charge fluctuations, dust fluid temperature, vortex-like ion distribution, strong dust correlation etc on the properties of dust ion-acoustic/dust-acoustic solitons have also been analysed. The implications of these theoretical investigations in experimental observations of soliton and shock formation in dusty plasmas are briefly discussed.

Contents

1. Introduction **2**
2. Basic equations **3**
3. Solitons **4**
3.1. DIA solitons 4
3.2. DA solitons 12
3.3. DL solitons 17
4. Shocks **22**
4.1. DIA shocks 22
4.2. DA shocks 27
5. Vortices **28**
5.1. Electrostatic vortices 29
5.2. Electromagnetic vortices 30
6. Discussion **33**
Acknowledgments **35**
References **35**

[1] Permanent address: Department of Physics, Jahangirnagar University, Savar, Dhaka, Bangladesh.

PII: S1367-2630(03)57124-5

1. Introduction

Charged dust particles are ubiquitous in most space [1]–[15] and laboratory plasmas [13], [16]–[18]. The charged dust particles introduce a great variety of new phenomena associated with waves and instabilities [7], [11]–[13], [19]–[37], and cause different interesting phenomena to occur in astrophysical and space environments, such as interplanetary space, interstellar medium, interstellar or molecular clouds, comets, planetary rings, earth's environments etc [1]–[6], [9]–[11], [13], [38]–[41].

The consideration of charged dust grains in a plasma not only modifies the existing plasma wave spectra [42]–[44], but it also introduces a number of new novel eigenmodes, such as dust ion-acoustic (DIA) waves [20, 26, 34], dust-acoustic (DA) waves [19, 25, 36], dust lattice (DL) waves [27, 31, 32, 35] etc in unmagnetized dusty plasma and dust drift (DD) mode [45], Shukla–Varma (SV) mode [46] and low-frequency electromagnetic modes (namely dust Alfvén waves, dust magnetosonic waves, mixed modes etc [7, 11, 13], [47]–[49]) in uniform/nonuniform dusty magnetoplasmas.

Shukla and Silin [20] first theoretically showed the existence of DIA waves. DIA waves have been observed in laboratory experiments [26, 34]. Rao *et al* [19] first theoretically predicted the existence of extremely low-phase-velocity (in comparison with the electron and ion thermal speeds) DA waves in an unmagnetized dusty plasma whose constituents are an inertial charged dust fluid and Boltzmann ions and electrons. Thus, in the DA waves the inertia is provided by the dust particle mass and the restoring force comes from the pressures of electrons and ions. The theoretical prediction of Rao *et al* [19] has been conclusively verified by a number of laboratory experiments [25, 36].

It is now well established that when the electrostatic energy of the dust particle interaction exceeds the kinetic energy, charged dust grains often form crystal-like structures [32], [50]–[54] in a strongly coupled dusty plasma. The waves associated with such strongly correlated dust crystals, which represent a unique object connecting plasma physics and condensed matter physics, cannot be explained in terms of DIA or DA wave theories. Melandsø [27] first presented a consistent theory for the DL waves by using the analytical expansion technique, previously known from solid state physics [55]. The theory of Melandsø [27], limited to only the interaction between nearest dust grains, was then improved by Farokhi *et al* [35] by taking into account the short- and long-range interactions between the dust particles.

These electrostatic modes usually exist in an unmagnetized dusty plasma. But, in practice, dusty plasma systems in most cases are confined in an external or self-generated magnetic field, and contain some region of inhomogeneity capable of causing drift motions and associated waves in a magnetized dusty plasma. Shukla *et al* [45] first considered a nonuniform magnetized dusty plasma and showed the existence of the DD mode. The dust-convective cells, which are now known as the SV mode [46], are also found to arise in the presence of an equilibrium density gradient and a uniform magnetic field. A number of authors, e.g. Shukla [7, 47], Shukla and Rahman [48], Birk *et al* [49], Verheest [11] etc, have also shown the existence of low-frequency electromagnetic waves (e.g. dust Alfvén waves, dust magnetosonic waves, mixed modes, etc) in uniform/nonuniform dusty magnetoplasmas.

The linear properties of DIA, DA, DL, SV and other low-frequency dust associated electrostatic and electromagnetic modes in dusty plasmas are now well understood and have been reported in a large number of regular and review articles or books over the last few years [7, 12, 13], [19]–[23], [25]–[28], [30]–[36], [46, 56, 57]. We know that the linear theories

are valid only when the wave amplitude is so small that one may neglect the nonlinearities. However, there are numerous processes via which unstable modes can saturate and attain large amplitudes. When the amplitudes of the waves are sufficiently large, we cannot neglect the nonlinearities. The nonlinearities contribute to the localization of waves and lead to different types of interesting nonlinear coherent structure, namely solitons, shocks, vortices etc. These nonlinear structures are very important from both theoretical and experimental points of view, and have received a great deal of attention for understanding the basic properties of localized electrostatic/electromagnetic perturbations in space and laboratory dusty plasmas.

Recently, a number of theoretical attempts have been made in order to study the properties of DIA solitons [13], [58]–[61] and shocks [13], [62]–[66], DA solitons [13, 19], [67]–[76] and shocks [12, 13, 61, 65], [77]–[79], DL solitons [27, 35] and vortices associated with low-frequency dust-associated electrostatic and electromagnetic waves [46], [80]–[82]. The DIA solitary [83] and shock waves [84]–[86] and DL solitary waves [87] have been experimentally observed.

In this paper, we present the underlying physics and the mathematical details of solitons, shocks and vortices in dusty plasmas. It is shown that the presence of dust particles introduces new aspects to the nonlinear waves and coherent structures. The manuscript is organized in the following fashion. We present our model equations in section 2. We study the properties of DIA, DA and DL solitons in section 3. We study DIA and DA shocks in section 44. We then consider nonuniform dusty magnetoplasma and analyse the electrostatic and electromagnetic vortices in section 5. We finally summarize our results in section 6.

2. Basic equations

We consider a multi-species dusty plasma containing electrons, ions and negatively charged dust grains. The macroscopic state of this dusty plasma system is described by

$$\frac{\partial N_j}{\partial t} + \nabla \cdot N_j \boldsymbol{U}_j = 0, \tag{1}$$

$$N_j m_j \left(\frac{\partial N_j}{\partial t} + \boldsymbol{U}_j \cdot \nabla \boldsymbol{U}_j \right) = q_j N_j \left(\boldsymbol{E} + \frac{1}{c} \boldsymbol{U}_j \times \boldsymbol{B} \right) - \nabla P_j, \tag{2}$$

$$\frac{\partial P_j}{\partial t} + \boldsymbol{U}_j \cdot \nabla P_j + \gamma P_j \nabla \cdot \boldsymbol{U}_j = 0, \tag{3}$$

$$\nabla \cdot \boldsymbol{E} = 4\pi \sum_j q_j N_j, \tag{4}$$

$$\nabla \times \boldsymbol{E} = -\frac{1}{c} \frac{\partial \boldsymbol{B}}{\partial t}, \tag{5}$$

$$\nabla \times \boldsymbol{B} = \frac{4\pi}{c} \sum_j q_j N_j U_j + \frac{1}{c} \frac{\partial \boldsymbol{E}}{\partial t}, \tag{6}$$

where j represents the species (i.e. $j = e$ for electrons, $j = i$ for ions and $j = d$ for dust particles), N_j is the number density, $\boldsymbol{U}_j$ is the fluid velocity, P_j is the fluid pressure, m_j is the mass, q_j is the charge (i.e. $q_e = -e$, $q_i = e$ and $q_d = -Z_d e$; here Z_d is the number of electrons residing on the dust grain surface and e is the charge of an electron), γ is the adiabatic index (which is 3 for the one-dimensional case and 5/3 in the three-dimensional case), $\boldsymbol{E}$ is the electric field, $\boldsymbol{B}$ is the magnetic field and c is the speed of light in vacuum.

3. Solitons

A soliton is a special type of solitary wave (a hump or dip shaped nonlinear wave of permanent profile) which preserves its shape and speed after collisions. It arises because of the balance between the effects of the nonlinearity and the dispersion (when the effect of dissipation is negligible in comparison with those of the nonlinearity and dispersion). Three types of soliton are found to exist in an unmagnetized dusty plasma. These are associated with three different classes of longitudinal electrostatic waves, namely DIA, DA and DL waves, and are known, respectively, as DIA, DA and DL solitons [13, 19, 58, 70, 77, 79, 80, 88]. These are described as follows.

3.1. DIA solitons

We confine ourself, in this section, to the DIA solitary waves in an unmagnetized dusty plasma in which dust particles are stationary and provide only the background charge neutrality. The basic equations (1)–(4) for one-dimensional DIA waves can be expressed in terms of normalized variables as

$$\frac{\partial n_i}{\partial t} + \frac{\partial}{\partial x}(n_i u_i) = 0, \tag{7}$$

$$\frac{\partial u_i}{\partial t} + u_i \frac{\partial u_i}{\partial x} = -\frac{\partial \phi}{\partial x} - \frac{\sigma_i}{n_i}\frac{\partial p_i}{\partial x}, \tag{8}$$

$$\frac{\partial p_i}{\partial t} + u_i \frac{\partial p_i}{\partial x} + 3p_i \frac{\partial u_i}{\partial x} = 0, \tag{9}$$

$$\frac{\partial^2 \phi}{\partial x^2} = \mu \exp(\phi) - n_i + (1-\mu), \tag{10}$$

where n_i is the ion number density normalized by its equilibrium value n_{i0}, u_i is the ion fluid velocity normalized by the ion-acoustic speed $C_i = (k_B T_e/m_i)^{1/2}$, $\sigma_i = T_i/T_e$, p_i is the ion pressure normalized by $n_{i0}k_B T_i$, ϕ is the ion-acoustic wave potential normalized by $K_B T_e/e$ and $\mu = n_{e0}/n_{i0}$. Here n_{e0} is the equilibrium electron number density, T_e (T_i) is the electron (ion) temperature and k_B is the Boltzmann constant. We have assumed a Boltzmannian electron density response, which is valid as long as $V_p \ll V_{Te}$.

The space variable x is normalized by the modified electron Debye radius $\lambda_{Dem} = (K_B T_e/4\pi n_{i0} e^2)^{1/2}$ and the time variable t is normalized by the ion plasma period $\omega_{pi}^{-1} = (m_i/4\pi n_{i0} e^2)^{1/2}$.

To obtain a solitary wave solution, we assume that all the dependent variables depend on a single independent variable $\xi = x - Mt$, where M is the Mach number (the velocity of the solitary wave normalized by the ion-acoustic speed C_i). Considering the steady state condition, i.e. $\partial/\partial t = 0$, we can write equations (7)–(10) as

$$M\frac{\partial n_i}{\partial \xi} - \frac{\partial}{\partial \xi}(n_i u_i) = 0, \tag{11}$$

$$M\frac{\partial u_i}{\partial \xi} - u_i \frac{\partial u_i}{\partial \xi} - \frac{\sigma_i}{n_i}\frac{\partial p_i}{\partial \xi} = \frac{\partial \phi}{\partial \xi}, \tag{12}$$

$$M\frac{\partial p_i}{\partial \xi} - u_i \frac{\partial p_i}{\partial \xi} - 3p_i \frac{\partial u_i}{\partial \xi} = 0, \tag{13}$$

$$\frac{\partial^2\phi}{\partial\xi^2} = \mu\exp(\phi) - n_i + (1-\mu). \tag{14}$$

Now, under the appropriate boundary conditions, namely $\phi \to 0$, $u \to 0$, $p_i \to 1$ and $n \to 1$ at $\xi \to \pm\infty$, equations (11) and (13) can be integrated to give

$$n_i = \frac{1}{1 - u_i/M}, \tag{15}$$

$$p_i = n_i^3. \tag{16}$$

Substituting equation (15) into (12) we obtain

$$M\frac{\partial u_i}{\partial\xi} - u_i\frac{\partial u_i}{\partial\xi} - \sigma_i\frac{\partial p_i}{\partial\xi} + \frac{\sigma_i}{M}u_i\frac{\partial p_i}{\partial\xi} = \frac{\partial\phi}{\partial\xi}. \tag{17}$$

Multiplying equation (13) by σ_i/M one can write

$$\sigma_i\frac{\partial p_i}{\partial\xi} - \frac{\sigma_i}{M}u_i\frac{\partial p_i}{\partial\xi} - 3p_i\frac{\sigma_i}{M}\frac{\partial u_i}{\partial\xi} = 0. \tag{18}$$

Now, subtracting equation (17) from (18) twice, one can get a differential equation which has the form

$$3\sigma_i\frac{\partial p_i}{\partial\xi} - 3\frac{\sigma_i}{M}\frac{\partial}{\partial\xi}(p_iu_i) - 2M\frac{\partial u_i}{\partial\xi} + 2u_i\frac{\partial u_i}{\partial\xi} + 2\frac{\partial\phi}{\partial\xi} = 0. \tag{19}$$

The integration of this equation yields

$$3\frac{\sigma_i}{M}p_iu_i - 3\sigma_i(p_i - 1) + 2Mu_i - u_i^2 - 2\phi = 0, \tag{20}$$

where we have used the same boundary conditions, namely $\phi \to 0$, $u_i \to 0$, $p_i \to 1$ and $n_i \to 1$ at $\xi \to \pm\infty$. Substituting u_i and p_i into equation (20) one can obtain a quadratic equation for n_i^2

$$3\sigma_i n_i^4 - (3\sigma_i + M^2 - 2\phi)n_i^2 + M^2 = 0. \tag{21}$$

The solution of equation (21) is given by

$$n_i = \frac{\sigma_{i1}}{\sqrt{2}\sigma_{i0}}\left[1 - \frac{2\phi}{M^2\sigma_{i1}^2} - \sqrt{\left(1 - \frac{2\phi}{M^2\sigma_{i1}^2}\right)^2 - 4\frac{\sigma_{i0}^2}{\sigma_{i1}^4}}\right]^{1/2}, \tag{22}$$

where $\sigma_{i0} = \sqrt{3\sigma_i/M^2}$ and $\sigma_{i1} = \sqrt{1+\sigma_{i0}^2}$. Substituting equation (22) into (14) and integrating the resultant equation, we have an energy integral [89, 90]

$$\frac{1}{2}\left(\frac{\mathrm{d}\phi}{\mathrm{d}\xi}\right)^2 + V(\phi) = 0, \tag{23}$$

where the pseudo-potential $V(\phi)$ is given by

$$V(\phi) = -\mu\exp(\phi) - -(1-\mu)\phi - \frac{M^2\sigma_{i1}}{\sqrt{2}}\left[1 - \frac{2\phi}{M^2\sigma_{i1}^2} + \sqrt{\left(1 - \frac{2\phi}{M^2\sigma_{i1}^2}\right)^2 - 4\frac{\sigma_{i0}^2}{\sigma_1^4}}\right]^{1/2}$$
$$- \frac{2\sqrt{2}\sigma}{\sigma_{i1}^3}\left[1 - \frac{2\phi}{M^2\sigma_{i1}^2} + \sqrt{\left(1 - \frac{2\phi}{M^2\sigma_{i1}^2}\right)^2 - 4\frac{\sigma_0^2}{\sigma_1^4}}\right]^{-3/2} + C_1. \tag{24}$$

Here C_1 is the integration constant which we will choose in such a manner that $V(\phi) = 0$ at $\phi = 0$. It is important to mention that in our study the condition for ion density to be real, $|1 - 2\phi/M^2\sigma_1^2| \geq 2\sigma_0/\sigma_1^2$, must always be satisfied.

To find the condition for the existence of DIA solitary waves analytically, we first consider the cold ion limit $\sigma_i = 0$ for which equation (24) reduces to

$$V(\phi) = \mu[1 - \exp(\phi)] - (1 - \mu)\phi + M^2\left(1 - \sqrt{1 - \frac{2\phi}{M^2}}\right). \tag{25}$$

It is obvious from equation (25) that $V(\phi) = \mathrm{d}V(\phi)/\mathrm{d}\phi = 0$ at $\phi = 0$. Therefore, solitary wave solutions of equation (25) exist if

(i) $(\mathrm{d}^2V/\mathrm{d}\phi^2)_{\phi=0} < 0$ so that the fixed point at the origin is unstable and

(ii) $(\mathrm{d}^3V/\mathrm{d}\phi^3)_{\phi=0} > (<)0$ for solitary waves with $\phi > (<)0$.

The nature of these solitary waves, whose amplitude tends to zero as the Mach number M tends to its critical value, can be found by expanding the Sagdeev potential $V(\phi)$ to third order in a Taylor series in ϕ. The critical Mach number is that which corresponds to the vanishing of the quadratic term. At the same time, if the cubic term is negative there is a potential well on the negative side, and if the cubic term is positive there is a potential well on the positive side. Therefore, by expanding the Sagdeev potential $V(\phi)$ around the origin, the critical Mach number at which the second derivative changes sign can be found as $M_c = \mu^{-1/2}$. At this critical value of M the cubic term of $V(\phi)$ can be expressed as $(3\mu - 1)\mu^{-1/2}/2$ which reveals that the cubic term is positive (negative) for $\mu > (<)1/3$. This means that depending on the value of μ, DIA solitary waves with both positive and negative potential can exist with $\phi > (<)0$ when $\mu > (<)1/3$.

To examine how the ion fluid temperature (σ_i) modifies the properties of the arbitrary amplitude DIA solitary waves, we have analysed the pseudo-potential $V(\phi)$ given by equation (24), and found that as we increase σ_i,

(i) we need higher values of the critical Mach number (corresponding to a lower value of μ) in order to have the DIA solitary waves, and

(ii) the amplitude of both the positive and negative solitary waves decreases, but their width increases.

We have also found the same results by numerical analysis of the energy integral (23). Since in most space and laboratory dusty plasmas $\mu < 1/3$, unlike the usual ion-acoustic solitary waves (associated with a positive potential) in a two-component electron–ion plasma [91] DIA solitary waves have a new feature in that these are associated with a negative potential which is due to the presence of negatively charged dust grains.

We have discussed the properties of the DIA solitary waves by assuming a planar geometry and constant dust grain charge. However, it is shown that the effects of nonplanar geometry and dust grain charge fluctuations introduce new features or significantly modify the properties of DIA solitary waves [13, 60, 61, 66]. We now consider the cold-ion limit ($\sigma_i = 0$) just to avoid mathematical complexities, and investigate the effects of nonplanar geometry and dust grain charge fluctuations on the properties of the DIA solitary waves.

3.1.1. Nonplanar geometry. The nonlinear dynamics of the DIA waves, whose phase speed is much smaller (larger) than the electron (ion) thermal speed (namely $V_{Ti} \ll V_p \ll V_{Te}$), in

nonplanar cylindrical and spherical geometries is governed by

$$\frac{\partial n_i}{\partial t} + \frac{1}{r^\nu}\frac{\partial}{\partial r}(r^\nu n_i u_i) = 0, \tag{26}$$

$$\frac{\partial u_i}{\partial t} + u_i\frac{\partial u_i}{\partial r} = -\frac{\partial \phi}{\partial r}, \tag{27}$$

$$\frac{1}{r^\nu}\frac{\partial}{\partial r}\left(r^\nu \frac{\partial \phi}{\partial r}\right) = \mu\exp(\phi) - n_i + (1-\mu), \tag{28}$$

where $\nu = 0$ for a one-dimensional geometry and $\nu = 1$ (2) for a non-planar cylindrical (spherical) geometry. We assumed here a constant dust grain charge (i.e. $Z_d = Z_{d0}$; here Z_{d0} is the equilibrium value of Z_d).

To investigate ingoing solutions of equations (26)–(28), we introduce stretched coordinates [92, 93] $\zeta = -\epsilon^{1/2}(r + v_0 t)$ and $\tau = \epsilon^{3/2}t$, expand n_i, u_i and ϕ in a power series of ϵ

$$n_i = 1 + \epsilon n_i^{(1)} + \epsilon^2 n_i^{(2)} + \cdots, \tag{29}$$

$$u_i = \epsilon u_i^{(1)} + \epsilon^2 u_i^{(2)} + \cdots, \tag{30}$$

$$\phi = \epsilon\phi^{(1)} + \epsilon^2\phi^{(2)} + \cdots \tag{31}$$

and develop equations in various powers of ϵ. To lowest order in ϵ, equations (26)–(31) give $n_i^{(1)} = -u_i^{(1)}/v_0$, $u_i^{(1)} = -\phi^{(1)}/v_0$ and $v_0 = \mu^{-1/2}$. To next higher order in ϵ, we obtain a set of equations

$$\frac{\partial n_i^{(1)}}{\partial \tau} - v_0\frac{\partial n_i^{(2)}}{\partial \zeta} - \frac{\partial u_i^{(2)}}{\partial \zeta} - \frac{\partial}{\partial \zeta}[n_i^{(1)}u_i^{(1)}] - \frac{\nu u_i^{(1)}}{v_0\tau} = 0, \tag{32}$$

$$\frac{\partial u_i^{(1)}}{\partial \tau} - v_0\frac{\partial u_i^{(2)}}{\partial \zeta} - u_i^{(1)}\frac{\partial u_i^{(1)}}{\partial \zeta} - \frac{\partial \phi^{(2)}}{\partial \zeta} = 0, \tag{33}$$

$$\frac{\partial^2 \phi^{(1)}}{\partial \zeta^2} - \mu\phi^{(2)} + n_i^{(2)} - \frac{1}{2}\mu[\phi^{(1)}]^2 = 0. \tag{34}$$

Combining equations (32)–(34) we deduce a modified Kortweg–de Vries (KdV) equation

$$\frac{\partial \phi^{(1)}}{\partial \tau} + \frac{\nu}{2\tau}\phi^{(1)} + A_g\phi^{(1)}\frac{\partial \phi^{(1)}}{\partial \zeta} + B_g\frac{\partial^3 \phi^{(1)}}{\partial \zeta^3} = 0, \tag{35}$$

where $A_g = (3\mu - 1)/\sqrt{2\mu}$ and $B_g = 1/2\mu^{3/2}$. We have already mentioned that $\nu = 0$ corresponds to a one-dimensional geometry. Thus, for a one-dimensional geometry ($\nu = 0$) and for a moving frame moving with a speed u_0, the stationary solitary wave solution of equation (35) is

$$\phi^{(1)}(\nu = 0) = \left(\frac{3u_0}{A_g}\right)\mathrm{sech}^2\left[\sqrt{\frac{u_0}{4B_g}}(\zeta - u_0\tau)\right]. \tag{36}$$

It is obvious from equation (36) that for $\mu > (<)\ 1/3$, a dusty plasma supports compressive (rarefactive) DIA solitary waves which are associated with a positive (negative) potential. We now turn to equation (35) with the term $(\nu/2\tau)\phi^{(1)}$ which is due to the effect of the nonplanar (cylindrical or spherical) geometry. An exact analytic solution of equation (35) is not possible. Therefore, we have numerically solved equation (35) and have studied the effects of cylindrical and spherical geometries on time-dependent DIA solitary waves. The results are depicted in figures 1 and 2. The initial condition that we have used in our numerical analysis is in the form of the stationary solution of equation (36) without the term $(\nu/2\tau)\phi$, i.e. in the form

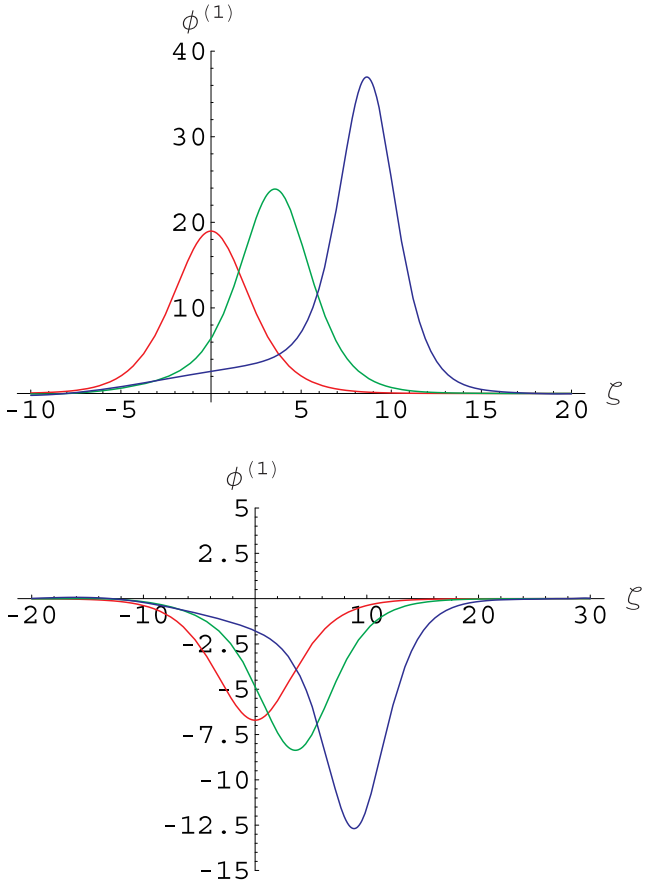

Figure 1. Time evolution of cylindrical ($\nu = 1$) DIA solitary waves: $\phi^{(1)}$ versus spatial coordinate ζ at times $\tau = -9$ (left), $\tau = -6$ (middle) and $\tau = -3$ (right) for $\mu = 0.4$ (upper plot) and $\mu = 0.2$ (lower plot). We choose our initial pulse at $\tau = -9$ and show how its amplitude increases with decreasing the value of τ (after [60]).

$\phi^{(1)} = (3/A_g)\text{sech}^2(\zeta/\sqrt{4B_g})$. Figure 1 shows how the effect of a cylindrical geometry modifies the DIA solitary waves associated with both positive ($\mu = 0.4 > 1/3$) and negative ($\mu = 0.2 < 1/3$) potentials. Figure 2 shows how the effect of a spherical geometry modifies the DIA solitary waves associated with both positive ($\mu = 0.4 > 1/3$) and negative ($\mu = 0.2 < 1/3$) potentials.

The numerical solutions of (35) (displayed in figures 1 and 2) reveal that for a large value of τ (e.g. $\tau = -9$) the spherical and cylindrical solitary waves are similar to one-dimensional solitary waves. This is because for a large value of τ the term $(\nu/2\tau)\phi^{(1)}$, which is due to the effect of the cylindrical or spherical geometry, is no longer dominant. However, as the value of τ decreases, the term $(\nu/2\tau)\phi^{(1)}$ becomes dominant and both spherical and cylindrical solitary waves differ from one-dimensional solitary waves. It is found that as the value of τ decreases, the amplitude of these localized pulses increases. It is also found that the amplitude of cylindrical solitary waves is larger than that of the one-dimensional solitary waves but smaller than that of the spherical ones.

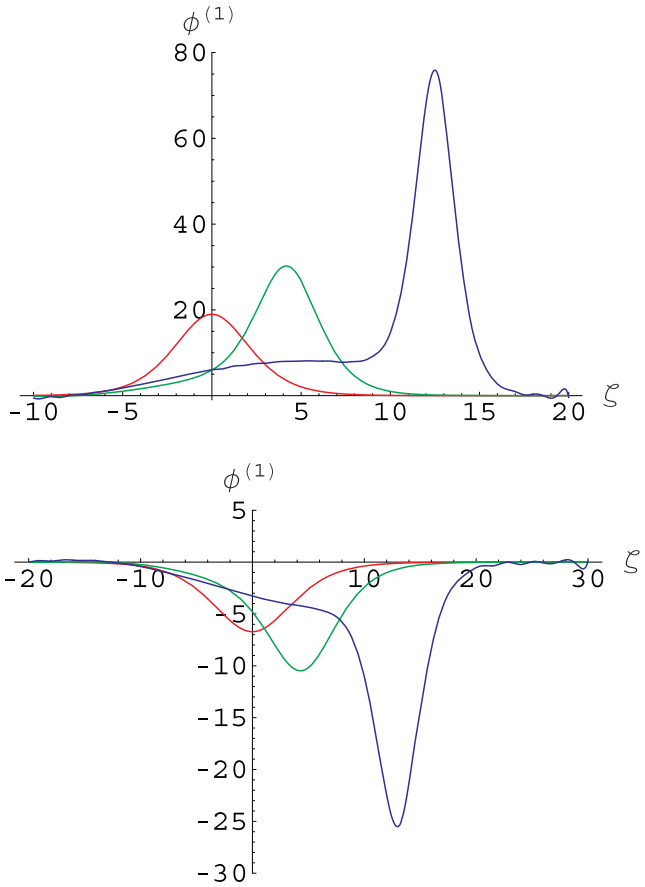

Figure 2. Time evolution of spherical ($\nu = 2$) DIA solitary waves: $\phi^{(1)}$ versus spatial coordinate ζ at times $\tau = -9$ (left), $\tau = -6$ (middle) and $\tau = -3$ (right) for $\mu = 0.4$ (upper plot) and $\mu = 0.2$ (lower plot). We choose our initial pulse at $\tau = -9$ and show how its amplitude increases with decreasing the value of τ (after [60]).

3.1.2. Dust charge fluctuations. We study the propagation of the DIA solitary waves in an unmagnetized dusty plasma where the dust charge is not constant but varies with space and time. The nonlinear dynamics of one-dimensional DIA waves, whose phase speed is much smaller (larger) than the electron (ion) thermal speed, is governed by equation (7) and

$$\frac{\partial u_i}{\partial t} + u_i \frac{\partial u_i}{\partial x} = -\frac{\partial \phi}{\partial x}, \tag{37}$$

$$\frac{\partial^2 \phi}{\partial x^2} = \mu \exp(\phi) - n_i + (1-\mu) z_d, \tag{38}$$

where z_d is the number of electrons residing on the dust grain surface normalized by its equilibrium value Z_{d0}. We note that z_d is not constant but varies with space and time. Thus, equations (7), (37) and (38) are completed by the normalized dust grain charging equation [13]

$$\eta \frac{\partial z_d}{\partial t} = \mu\beta \exp(\phi - \alpha z_d) - \beta_i n_i u_i \left(1 + \frac{2\alpha z_d}{u_i^2}\right), \tag{39}$$

where $\eta = \sqrt{\alpha m_e(1-\mu)/2m_i}$, $\alpha = Z_{d0}e^2/k_BT_er_d$, $\beta = (r_d/a)^{3/2}$, $a = n_{d0}^{-1/3}$ and $\beta_i = \beta\sqrt{\pi m_e/8m_i}$. We note that at equilibrium $\mu\beta\exp(-\alpha) = \beta_i u_0(1+2\alpha/u_0^2)$, where u_0 is the ion streaming speed normalized by C_i.

To study small but finite amplitude DIA solitary waves, we first introduce stretched coordinates [92] $\xi = \epsilon^{1/2}(x - v_0t)$, $\tau = \epsilon^{3/2}t$ and $\eta = \epsilon\eta_0$, where ϵ is the expansion parameter, measuring the amplitude of the wave or the weakness of the wave dispersion. We then expand n_i, u_i, ϕ and z_d in a power series of ϵ

$$n_i = 1 + \epsilon n_i^{(1)} + \epsilon^2 n_i^{(2)} + \cdots, \tag{40}$$

$$u_i = u_0 + \epsilon u_i^{(1)} + \epsilon^2 u_i^{(2)} + \cdots, \tag{41}$$

$$\phi = \epsilon\phi^{(1)} + \epsilon^2\phi^{(2)} + \cdots, \tag{42}$$

$$z_d = 1 + \epsilon z_d^{(1)} + \epsilon^2 z_d^{(2)} + \cdots. \tag{43}$$

We develop the equations in powers of ϵ. To lowest order in ϵ, equations (7) and (37)–(39) give

$$w_0 n_i^{(1)} = u_i^{(1)}, \tag{44}$$

$$w_0 u_i^{(1)} = \phi^{(1)}, \tag{45}$$

$$0 = \mu\phi^{(1)} - n_i^{(1)} + (1-\mu)z_d^{(1)}, \tag{46}$$

$$0 = \beta_e\phi^{(1)} - \alpha u_\beta z_d^{(1)} - \beta_i u_1 u_i^{(1)} - u_0\beta_i u_2 n_i^{(1)}, \tag{47}$$

where $w_0 = v_0 - u_0$, $u_1 = 1 - 2\alpha/u_0$, $u_2 = 1 + 2\alpha/u_0^2$, $u_\beta = \beta_e + 2\beta_i/u_0$ and $\beta_e = \mu\beta\exp(-\alpha)$. Now, substituting $n_i^{(1)}$, $u_i^{(1)}$ and $z_d^{(1)}$ (obtained from equations (44), (45) and (47)) into (46), we obtain the dispersion relation

$$aw_0^2 - bw_0 - c = 0, \tag{48}$$

where

$$a = \mu + \frac{(1-\mu)\beta_e}{\alpha u_\beta}, \tag{49}$$

$$b = \frac{(1-\mu)u_1\beta_i}{\alpha u_\beta}, \tag{50}$$

$$c = 1 + \frac{(1-\mu)u_2u_0\beta_i}{\alpha u_\beta}. \tag{51}$$

To next higher order in ϵ, from equations (7) and (37)–(39) we obtain a set of equations

$$\frac{1}{w_0^2}\frac{\partial\phi^{(1)}}{\partial\tau} - w_0\frac{\partial n_i^{(2)}}{\partial\xi} + \frac{\partial u_i^{(2)}}{\partial\xi} + \frac{2}{w_0^3}\phi^{(1)}\frac{\partial\phi^{(1)}}{\partial\xi} = 0, \tag{52}$$

$$\frac{1}{w_0}\frac{\partial\phi^{(1)}}{\partial\tau} - w_0\frac{\partial u_i^{(2)}}{\partial\xi} + \frac{1}{w_0^2}\phi^{(1)}\frac{\partial\phi^{(1)}}{\partial\xi} = \frac{\partial\phi^{(2)}}{\partial\xi}, \tag{53}$$

$$\frac{\partial^2\phi^{(1)}}{\partial\xi^2} = \mu\phi^{(2)} + \frac{1}{2}\mu[\phi^{(1)}]^2 - n_i^{(2)} + (1-\mu)z_d^{(2)}, \tag{54}$$

$$0 = \beta_e\phi^{(2)} - \alpha u_\beta z_d^{(2)} - \beta_i u_1 u_i^{(2)} - u_0\beta_i u_2 n_i^{(2)} + \beta_1\phi^{(1)}\frac{\partial\phi^{(1)}}{\partial\xi}, \tag{55}$$

where

$$\beta_1 = \beta_e[1 + (\alpha\beta_0 - 2)\alpha\beta_0] - \frac{2\beta_i}{w_0^3}\left[1 + \frac{w_\alpha}{u_0^3}\right], \tag{56}$$

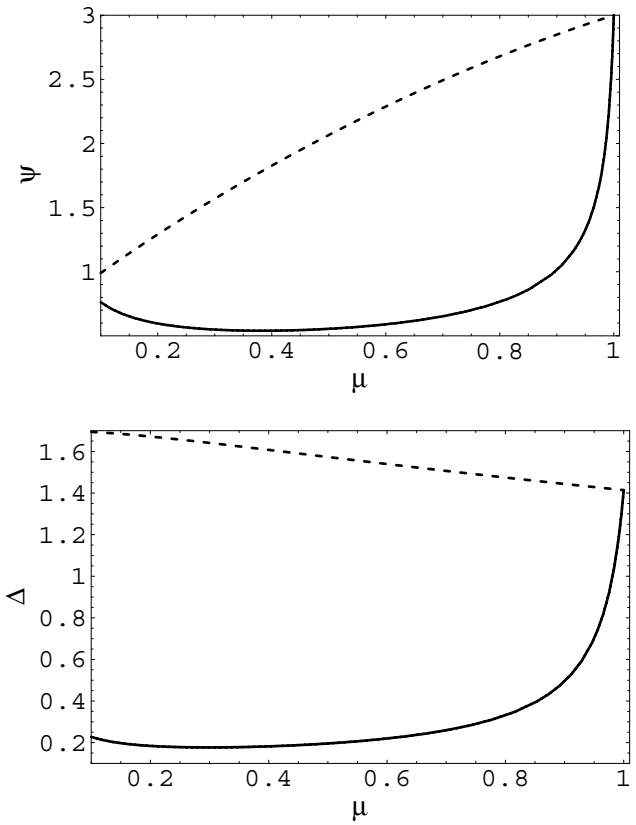

Figure 3. Variation of the amplitude ψ (upper plot) and the width Δ of the solitary waves with μ for $U_0 = 1$. The solid curves correspond to space dusty plasma parameters, $\alpha = 0.0288$ and $\beta = 3 \times 10^{-10}$, whereas the dotted curves correspond to laboratory dusty plasma parameters, $\alpha = 1.44$ and $\beta = 3 \times 10^{-4}$ (after [66]).

$$\beta_0 = \frac{1}{\alpha u_\beta}\left[\beta_e - \frac{\beta_i w_2}{w_0} + \frac{2\alpha\beta_i}{w_0 u_0}\left(1 - \frac{1}{w_0}\right)\right], \tag{57}$$

$w_1 = 1 - u_0/w_0$, $w_2 = 1 + u_0/w_0$ and $w_\alpha = 2\alpha w_0 w_1(1 - \beta_0 w_0 u_0)$. Now, combining equations (52)–(55) we deduce a KdV equation

$$\frac{\partial\phi^{(1)}}{\partial\tau} + A_c\phi^{(1)}\frac{\partial\phi^{(1)}}{\partial\xi} + B_c\frac{\partial^3\phi^{(1)}}{\partial\xi^3} = 0, \tag{58}$$

where

$$A_c = \frac{3c + bw_0 - \beta_2 w_0^4}{w_0(2c + bw_0)}, \tag{59}$$

$$B_c = \frac{w_0^3}{2c + bw_0}, \tag{60}$$

$$\beta_2 = \mu + \frac{\beta_1(1 - \mu)}{\alpha u_\beta}. \tag{61}$$

The stationary solution of the KdV equation (58) is obtained by transforming the independent variables ξ to $\zeta = \xi - U_0\tau$, where U_0 is a constant speed normalized by C_i, and imposing the

appropriate boundary conditions for localized perturbations, namely $\phi^{(1)} \to 0$, $\mathrm{d}\phi^{(1)}/\mathrm{d}\zeta \to 0$ and $\mathrm{d}^2\phi^{(1)}/\mathrm{d}\zeta^2 \to 0$ at $\zeta \to \pm\infty$. Accordingly, the stationary solitary wave solution of equation (58) is

$$\phi^{(1)} = \psi \ \mathrm{sech}^2[(\xi - U_0\tau)/\Delta], \tag{62}$$

where $\psi = 3U_0/A_c$ and $\Delta = \sqrt{4B_c/U_0}$ represent the amplitude and the width of the solitary waves, respectively. It is obvious from (62) that there exist compressive (rarefactive) solitary waves if $A_c > 0$ ($A_c < 0$). We have numerically analysed ψ and Δ for the parameters corresponding to space dusty plasma parameters, $n_{d0} = 10^{-7}$ cm^{-3}, $r_d = 1$ μm, $k_BT_e = 50$ eV and $Z_{d0} = 10^3$ [6, 13], which correspond to $\alpha = 0.0288$ and $\beta = 3 \times 10^{-10}$, as well as laboratory dusty plasma parameters, $n_{d0} = 10^5$ cm^{-3}, $r_d = 5$ μm, $k_BT_e = 0.2$ eV and $Z_{d0} = 10^3$ [26, 34], which correspond to $\alpha = 1.44$ and $\beta = 3 \times 10^{-4}$. We found that ψ is always positive (which is obvious from the upper plot of figure 3, since $U_0 > 0$). This means that our present dusty plasma model can only support compressive solitary waves (solitary waves with $\phi > 0$). The results of our numerical analyses (cf figure 3) show how the amplitude and the width of these compressive solitary waves vary with μ for both the space [6, 13] and laboratory [26, 34] dusty plasma situations.

3.2. DA solitons

We consider here the dynamics of negatively charged dust particles, and study the nonlinear behaviour of the DA waves whose phase speed is much smaller than the electron and ion thermal speeds, namely $V_p \ll V_{Te}, V_{Ti}$. The nonlinear dynamics of DA solitary waves in a one-dimensional unmagnetized dusty plasma system with a constant dust grain charge is thus governed by [19]

$$\frac{\partial n_d}{\partial t} + \frac{\partial}{\partial z}(n_d u_d) = 0, \tag{63}$$

$$\frac{\partial u_d}{\partial t} + u_d\frac{\partial u_d}{\partial z} = \frac{\partial \varphi}{\partial z} - \frac{\sigma_d}{n_d}\frac{\partial p_d}{\partial z}, \tag{64}$$

$$\frac{\partial p_d}{\partial t} + u_d\frac{\partial p_d}{\partial z} + 3p_d\frac{\partial u_d}{\partial z} = 0, \tag{65}$$

$$\frac{\partial^2 \varphi}{\partial z^2} = n_d + \mu_e \exp(\sigma_i\varphi) - \mu_i \exp(-\varphi), \tag{66}$$

where n_d is the particle number density normalized by its equilibrium value n_{d0}, u_d is the dust fluid velocity normalized by $C_d = (Z_{d0}k_BT_i/m_d)^{1/2}$ and φ is the electrostatic wave potential normalized by k_BT_i/e, p_d is the dust fluid pressure normalized by $n_{d0}k_BT_d$, $\sigma_d = T_d/Z_dT_i$, T_d is the dust fluid temperature, $\mu_e = n_{e0}/Z_{d0}n_{d0} = \mu/(1-\mu)$ and $\mu_i = n_{i0}/Z_{d0}n_{d0} = 1/(1-\mu)$. The time ($t$) and space ($z$) variables are in units of the dust plasma period $\omega_{pd}{}^{-1} = (m_d/4\pi n_{d0}Z_{d0}^2e^2)^{1/2}$ and the Debye length $\lambda_{Dim} = (k_BT_i/4\pi Z_{d0}n_{d0}e^2)^{1/2}$, respectively.

To study arbitrary amplitude DA solitary waves in such a dusty plasma system, we assume that all the dependent variables depend on a single independent variable $\xi = z - Mt$ and reduce equation (63)–(66) to an energy integral (by following the mathematical procedure presented in section 3)

$$\frac{1}{2}\left(\frac{\mathrm{d}\varphi}{\mathrm{d}\xi}\right)^2 + V(\varphi) = 0, \tag{67}$$

where the pseudo-potential potential $V(\varphi)$ is

$$V(\varphi) = -\left(\frac{\mu_e}{\sigma_i}\right)\exp(\sigma_i\varphi) - \mu_i\exp(-\varphi) - M^2\sqrt{\sigma_{d0}}\left[e^{\theta/2} + \frac{1}{3}e^{-3\theta/2}\right] + C_1, \tag{68}$$

with

$$\theta = \cosh^{-1}\left[\frac{\sigma_{d1}^2}{2\sigma_{d0}}\left(1 + \frac{2\varphi}{M^2\sigma_{d1}^2}\right)\right], \tag{69}$$

$\sigma_{d0} = \sqrt{3\sigma_d/M^2}$, $\sigma_{d1} = \sqrt{1+\sigma_{d0}^2}$ and C_1 is an integration constant. The latter is determined from $V(\varphi) = 0$ at $\varphi = 0$. It is important to note that we cannot consider the limit $\sigma_d \to 0$ in the Sagdeev potential $V(\varphi)$ in its present form. To consider the limit $\sigma_d \to 0$, we express θ as

$$\theta = \ln\left[\frac{\sigma_{d1}^2}{2\sigma_{d0}}\left(1 + \frac{2\varphi}{M^2\sigma_{d1}^2}\right) + \sqrt{\frac{\sigma_{d1}^4}{4\sigma_{d0}^2}\left(1 + \frac{2\varphi}{M^2\sigma_{d1}^2}\right)^2 - 1}\right]. \tag{70}$$

We note that in our study the condition for the dust density to be real requires $|1 + 2\varphi/M^2\sigma_{d1}^2| \geq 2\sigma_{d0}/\sigma_{d1}^2$. To find the condition for the existence of DA solitary waves analytically, we first consider the cold ion limit $\sigma_d = 0$ for which equation (70) reduces to the form [70]

$$V(\varphi) = \mu_i[1 - \exp(-\varphi)] + \frac{\mu_e}{\sigma_i}[1 - \exp(\sigma_i\varphi)] + M^2\left[1 - \left(1 + \frac{2\varphi}{M^2}\right)^{1/2}\right]. \tag{71}$$

It is obvious from equation (71) that $V(\varphi) = \mathrm{d}V(\varphi)/\mathrm{d}\varphi = 0$ at $\varphi = 0$. Therefore, solitary wave solutions of equation (67) exist if

(i) $(\mathrm{d}^2V/\mathrm{d}\varphi^2)_{\varphi=0} < 0$ so that the fixed point at the origin is unstable and

(ii) $(\mathrm{d}^3V/\mathrm{d}\varphi^3)_{\varphi=0} > (<)0$ for solitary waves with $\varphi > (<)0$.

The nature of these solitary waves, whose amplitude tends to zero as the Mach number M tends to its critical value, can be found by expanding the Sagdeev potential $V(\varphi)$ to third order in a Taylor series in φ. The critical Mach number is that which corresponds to the vanishing of the quadratic term. At the same time, if the cubic term is negative, there is a potential well on the negative side, and if the cubic term is positive, there is a potential well on the positive side. Therefore, by expanding the Sagdeev potential $V(\varphi)$ around the origin, the critical Mach number at which the second derivative changes sign can be found as $M_c = \sqrt{(1-\mu)/(1+\sigma_i\mu)}$. Figure 4 depicts the variation of the critical Mach number M_c against n_{e0}/n_{i0} $(= \mu)$ for different values of σ_i. The figure shows that the critical Mach number increases with σ_i, but decreases with μ. At the critical value of M the cubic term of $V(\varphi)$ can be expressed as $-[1+(3+\sigma_i\mu)\sigma_i\mu+\mu(1+\sigma_i^2)/2]/[3(1-\mu)^2]$. This clearly reveals that the cubic term is always negative for any value of σ_i and μ, i.e. only DA solitary waves with $\varphi < 0$ can exist.

It is of interest to examine whether or not there exists an upper limit of M for which DA solitary waves can exist. This upper limit of M can be found by the condition $V(\varphi_c) \geq 0$, where $\varphi_c = -M^2/2$ is the minimum value of φ for which the dust number density n_d is real. Thus, the upper limit of M is that maximum value of M for which $S_m \geq 0$, where $S_m = \mu_i + \mu_e/\sigma_i + M^2 - \mu_i\exp(M^2/2) - (\mu_e/\sigma_i)\exp(-\sigma_i M^2/2)$. Figure 5 shows the variation of S_m against M for different values of μ. We notice that as we increase μ, the upper limit of M decreases. We note that for $\sigma_i = 0.05$ and $\mu = 0.1$, there exist DA solitary waves with $\varphi < 0$ for $0.95 < M < 1.52$. We have also numerically analysed the Sagdeev potential $V(\varphi)$

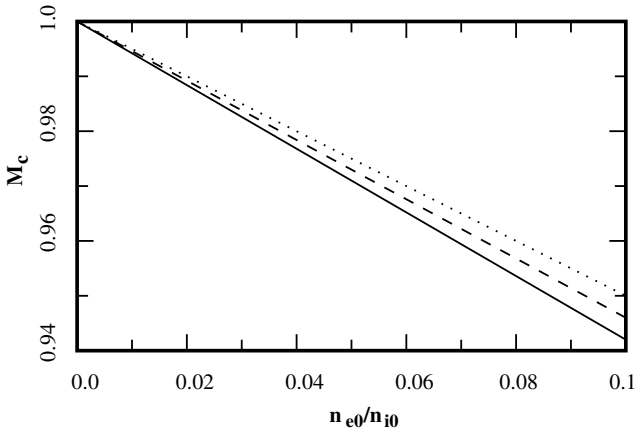

Figure 4. Variation of the critical Mach number M_c against n_{e0}/n_{i0} for $\sigma_i = 0.01$ (solid curve), $\sigma_i = 0.05$ (dashed curve) and $\sigma_i = 0.1$ (dotted curve) (after [70]).

and have found the same results, that for $\sigma_i = 0.05$ and $\mu = 0.1$ there exists a potential well on the negative φ-axis for $0.95 < M < 1.52$, i.e. there exist DA solitary waves with $\varphi < 0$ for $0.95 < M < 1.52$ (for details we refer to [70]).

To examine how the dust fluid temperature (σ_d) modifies the properties of the arbitrary amplitude DA solitary waves, we analyse the pseudo-potential potential $V(\varphi)$ given by equation (68), and find that as we increase σ_d,

(i) we need a higher value of the Mach number in order to have solitary wave solutions of equation (67), and

(ii) the amplitude of the solitary waves decreases, but their width increases.

We have also found the same results by numerical analysis of the energy integral (67). The potential profiles, as solutions of equation (67), are displayed in figure 6, showing the effects of dust temperature on their amplitude and width.

We have discussed the properties of the DA solitary waves by assuming a planar geometry and Maxwellian ion distribution. However, it can be shown that the effects of non-planar geometry and non-Maxwellian ion distribution introduce new features or significantly modify the properties of the DA solitary waves [13, 66, 68, 74]. We now consider the cold-dust limit ($\sigma_d = 0$) just to avoid the mathematical complexities, and investigate the effects of a non-Maxwellian (vortex-like) ion distribution and non-planar geometry on the properties of the DA solitary waves.

3.2.1. Vortex-like ion distribution. It is well known [94]–[97] that the electron and ion distribution functions can be significantly modified in the presence of large-amplitude waves that are excited by the two-stream instability [24]. Accordingly, the electron and ion number densities depart from a Boltzmann distribution when a phase space vortex distribution appears in a plasma. For the DA waves, the ion trapping in the wave potential is our interest. To study the effects of non-isothermal ions on the DA solitary waves, we consider the trapped or vortex-like [94, 95] ion distribution $f_i = f_{if} + f_{it}$, where

$$f_{if} = \frac{1}{\sqrt{2\pi}} \exp\left[-\frac{1}{2}(v_i^2 + 2\varphi)\right] \tag{72}$$

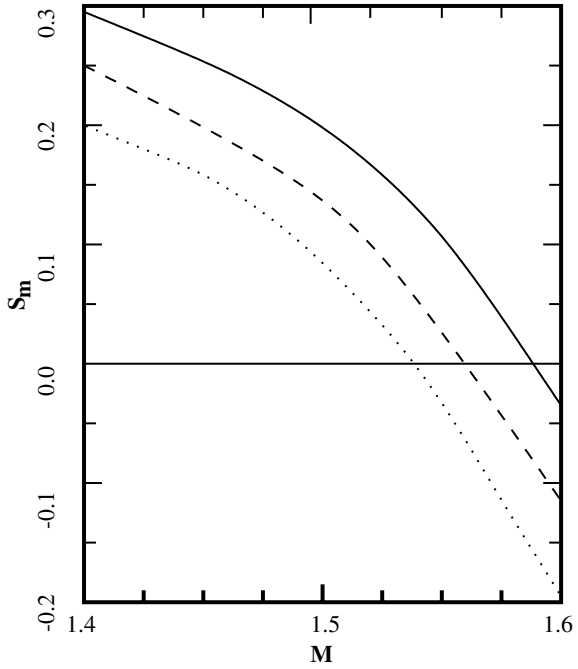

Figure 5. Variation of S_m against M for $\sigma_i = 0.05$, $\mu = 0$ (solid curve), $\mu = 0.05$ (dashed curve) and $\mu = 0.1$ (dotted curve). The upper limit of M is that value for which $S_m = 0$ (after [70]).

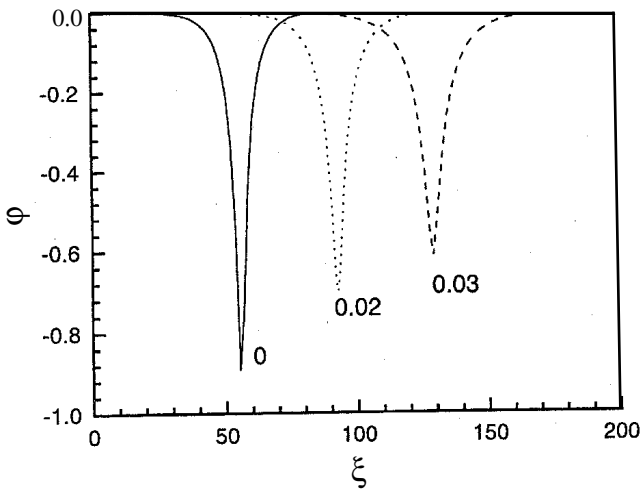

Figure 6. Potential profiles for $\sigma_i = 0.2$, $\mu = 0.1$, $M = 1.455$ and $\sigma_d = 0$ (solid curve), $\sigma_d = 0.02$ (dotted curve) and $\sigma_d = 0.03$ (dashed curve) (after [13]).

for $|v_i| > \sqrt{-2\varphi}$ and

$$f_{it} = \frac{1}{\sqrt{2\pi}} \exp\left[-\frac{1}{2}\sigma_{it}(v_i^2 + 2\varphi)\right] \tag{73}$$

for $|v_i| \leq \sqrt{-2\varphi}$. We note that the ion distribution function, as prescribed above, is continuous in velocity space and satisfies the regularity requirements for an admissible BGK solution [89].

Here the ion velocity v_i in equations (72) and (73) is normalized by the ion thermal speed V_{Ti}, and $\sigma_{it} = T_i/T_{it}$, the ratio of the free ion temperature T_i to the trapped ion temperature T_{it}, is a parameter determining the number of trapped ions. Integrating the ion distributions over velocity space we readily obtain the ion number density n_i as [96]

$$n_i = I(-\varphi) + \frac{1}{\sqrt{\sigma_{it}}} \exp(-\sigma_{it}\varphi)\mathrm{erf}(\sqrt{-\sigma_{it}\varphi}) \tag{74}$$

for $\sigma_{it} > 0$ and

$$n_i = I(-\varphi) + \frac{1}{\sqrt{\pi\,|\sigma_{it}|}} W_D(\sqrt{\sigma_{it}\varphi}) \tag{75}$$

for $\sigma_{it} < 0$, where

$$I(z_0) = [1 - \mathrm{erf}(\sqrt{z_0})]\exp(z_0), \tag{76}$$

$$\mathrm{erf}(z_0) = \frac{2}{\sqrt{\pi}} \int_0^{z_0} \exp(-y^2)\,\mathrm{d}y, \tag{77}$$

$$W_D(z_0) = \exp(-z_0^2) \int_0^{z_0} \exp(y^2)\,\mathrm{d}y. \tag{78}$$

If we expand n_i in the small-amplitude limit (namely $\varphi \ll 1$) and keep terms up to φ^2, it is found that n_i is the same for both $\sigma_{it} < 0$ and $\sigma_{it} > 0$. It is expressed as

$$n_i \simeq 1 - \varphi - \frac{4(1-\sigma_{it})}{3\sqrt{\pi}}(-\varphi)^{3/2} + \frac{1}{2}\varphi^2. \tag{79}$$

We now follow the reductive perturbation technique of Schamel and construct a weakly nonlinear theory for DA solitary waves by introducing the stretched coordinates $\zeta = \epsilon^{1/4}(z - v_0 t)$ and $\tau = \epsilon^{3/4} t$. Using equations (63) and (66) with $\sigma_d = 0$ and equation (72) with the replacement of $\mu_i \exp(-\varphi)$ by the right-hand side of equation (79), and applying the reductive perturbation technique of [95], we can derive

$$\frac{\partial \varphi^{(1)}}{\partial \tau} + a_t \sqrt{-\varphi^{(1)}} \frac{\partial \varphi^{(1)}}{\partial \zeta} + b_s \frac{\partial^3 \varphi^{(1)}}{\partial \zeta^3} = 0, \tag{80}$$

where

$$a_t = \frac{v_0^3(1-\sigma_{it})}{\sqrt{\pi}(1-\mu)}. \tag{81}$$

Equation (80) is a modified KdV equation exhibiting a stronger nonlinearity, smaller width and larger propagation speed of the DA solitary waves.

The stationary soliton-like solution of the modified KdV equation (80) can be obtained by transforming the space variable ζ to $\eta = \zeta - u_0\tau$ and by imposing the appropriate boundary conditions, namely $\varphi \to 0$, $\mathrm{d}\varphi^{(1)}/\mathrm{d}\eta \to 0$ and $\mathrm{d}^2\varphi^{(1)}/\mathrm{d}\eta^2 \to 0$ at $\eta \to \pm\infty$. Thus, the stationary solution of equation (80) can be expressed as

$$\varphi^{(1)} = -\varphi_m^{(1)} \mathrm{sech}^4[(\zeta - u_0\tau)/\Delta_t], \tag{82}$$

where the amplitude $\varphi_m^{(1)}$ and the width Δ_t are given by $\varphi_m^{(1)} = (15u_0/8a_t)^2$ and $\Delta_t = \sqrt{16b_s/u_0}$, respectively. As $u_0 > 0$ and $\mu < 1$, equation (82) reveals that there exist solitary waves with negative potential only. It is also observed that as u_0 increases, the amplitude increases while the width decreases.

3.2.2. Nonplanar geometry. It is well known that in laboratory devices one may encounter multi-dimensional DA solitary waves. We are, therefore, interested in examining radially ingoing DA solitary waves in nonplanar (cylindrical and spherical) geometries. The dynamics of low-phase-velocity nonlinear DA waves in cylindrical and spherical geometries are governed by [93]

$$\frac{\partial n_d}{\partial t} + \frac{1}{r^\nu}\frac{\partial}{\partial r}(r^\nu n_d u_d) = 0, \tag{83}$$

$$\frac{\partial u_d}{\partial t} + u_d\frac{\partial u_d}{\partial r} = \frac{\partial \varphi}{\partial r}, \tag{84}$$

$$\frac{1}{r^\nu}\frac{\partial}{\partial r}\left(r^\nu \frac{\partial \varphi}{\partial r}\right) = n_d + \mu_e \exp(\sigma_i \varphi) - \mu_i \exp(-\varphi), \tag{85}$$

where $\nu = 1, 2$ for cylindrical and spherical geometries, respectively. The space variable r is normalized by the Debye radius λ_{Ddm}.

To investigate ingoing solutions of equations (83)–(85), we introduce the stretched coordinates [93] $\zeta = -\epsilon^{1/2}(r + v_0 t)$ and $\tau = \epsilon^{3/2}t$, expand n_d, u_d and φ in powers of ϵ and develop equations in various powers of ϵ. Thus, performing all the mathematical steps as in the case of cylindrical or spherical DIA waves, one can deduce a modified KdV equation

$$\frac{\partial \varphi^{(1)}}{\partial \tau} + \frac{\nu}{2\tau}\varphi^{(1)} - A_{gd}\varphi^{(1)}\frac{\partial \varphi^{(1)}}{\partial \zeta} + B_{gd}\frac{\partial^3 \varphi^{(1)}}{\partial \zeta^3} = 0, \tag{86}$$

where

$$A_{gd} = \frac{v_0^3}{(1-\mu)^2}\left[1 + (3 + \sigma_i\mu)\sigma_i\mu + \frac{1}{2}\mu(1 + \sigma_i^2)\right], \tag{87}$$

and $B_{gd} = v_0^3/2$. If we compare equation (86) with equation (13) of [70], it is obvious that the term $(\nu/2\tau)\varphi^{(1)}$ in equation (86) is due to the effect of the cylindrical or spherical geometry. Using the same numerical method as we used in order to study cylindrical and spherical DIA solitary waves, we numerically solve equation (86) and study the effects of cylindrical and spherical geometries on time-dependent DA solitary waves. The numerical results (for details we refer [74]) reveal that for a large value of τ (e.g. $\tau = -31.6$) the spherical and cylindrical solitary waves are similar to one-dimensional solitary waves. This is because for a large value of τ the term $(\nu/2\tau)\varphi^{(1)}$, which is due to the effect of the cylindrical or spherical geometry, is no longer dominant. However, as the value of τ decreases, the term $(\nu/2\tau)\varphi^{(1)}$ becomes dominant and both spherical and cylindrical solitary waves differ from one-dimensional solitary waves. It is also found that as the value of τ decreases, the amplitude of these localized pulses increases.

3.3. DL solitons

Melandsø [27] first presented a consistent theory for longitudinal DL solitary waves. The theory of Melandsø [27], which is limited to the interaction between nearest dust grains (to be discussed later), was then improved by Farokhi *et al* [35] who took into account the short- and long-range interactions between the dust particles. We now study the properties of small- but finite-amplitude DL solitary waves by summarizing the works of [35, 57].

We consider a multi-component dusty plasma in which extremely massive, negatively charged dust grains are considered as discrete particles, and electrons and the ions are assumed

to be Boltzmannian (i.e. $N_e = n_{e0}\exp(e\Phi/k_BT_e)$ and $N_i = n_{i0}\exp(-e\Phi/k_BT_i)$. The ambipolar potential Φ satisfies Poisson's equation

$$\nabla^2\Phi - 4\pi e[n_{e0}\exp(e\Phi/k_BT_e) - n_{i0}\exp(-e\Phi/k_BT_i)] = -\sum_n q_n(\boldsymbol{r}, \Phi), \quad (88)$$

where the space charge contributions from all dust particles are included by the right-hand side term. The space charge density, corresponding to the nth spherical grain of radius r_{dn}, can be represented as

$$q_n(\boldsymbol{r}, \Phi) = \frac{Q_n}{4\pi r_{dn}^2}\int_{S_n} \mathrm{d}S\,\hat{\boldsymbol{n}}\delta(\boldsymbol{r} - [\boldsymbol{r}_n + r_{dn}\hat{\boldsymbol{n}}]), \quad (89)$$

where S_n is the surface area of the nth grain, $\boldsymbol{r}_n$ is the radius vector of the grain, $\hat{\boldsymbol{n}}$ a unit vector perpendicular to the surface element $\mathrm{d}S$ and Q_n denotes the total charge of the grain. Assuming that the grains are conductors, we have $Q_n = r_{dn}\phi(\boldsymbol{r}_n)$. When the dust grain radius r_d is assumed to be much smaller than the intergrain distance a (i.e. $r_d \ll a$), we can neglect the last term in the argument of the δ-function, and from equation (89) we then obtain

$$q_n(\boldsymbol{r}, \Phi) = Q_n\delta(\boldsymbol{r} - \boldsymbol{r}_n) = r_{dn}\delta(\boldsymbol{r} - \boldsymbol{r}_n)\Phi(\boldsymbol{r}). \quad (90)$$

Thus, substituting equation (90) into equation (88), and assuming $\Phi/k_BT_e \ll 1$ and $\Phi/k_BT_i \ll 1$, we have a Schrödinger type equation

$$\nabla^2\Phi + [-k_D^2 - V(\boldsymbol{r})]\Phi = 0, \quad (91)$$

$$V(\boldsymbol{r}) = -\sum_n r_{dn}\delta(\boldsymbol{r} - \boldsymbol{r}_n). \quad (92)$$

We note that equation (91) is often used in solid state physics for the description of lattice waves in the one-dimensional approximation [55]. Equation (91) for the one-dimensional case can be written as

$$\frac{\partial^2\Phi(z)}{\partial z^2} - k_D^2\Phi(z) + \sum_n b_n\delta(z - z_n)\Phi(z) = 0, \quad (93)$$

where $b_n = N_0 r_{dn}/S$ is the size of the dust grain, averaged over the area S perpendicular to the linear lattice, and N_0 the number of the dust grains embraced by the area S. Equation (93) determines the real potential Φ and the condition of the periodicity (for the ideal lattice) cannot contain an exponential factor (the Bloch coefficient), as happens in solid state physics. The solutions of (93) are

$$\Phi(z) = A_n\sinh[k_D(z - z_n)] + B_n\cosh[k_D(z - z_n)] \quad (94)$$

for $z_n < z < z_{n+1}$ and

$$\Phi(z) = A_{n-1}\sinh[k_D(z - z_{n-1})] + B_{n-1}\cosh[k_D(z - z_{n-1})] \quad (95)$$

for $z_{n-1} < z < z_n$. Obviously, $B_n = \Phi(z_n) = \Phi_n$, where Φ_n is the potential of the nth grain, and Φ_n is assumed to be known.

The solution of equation (93) and its derivative must satisfy two boundary conditions, namely

$$\Phi(z)|_{z_n+0} = \Phi|_{z_n-0}, \quad (96)$$

$$\frac{\partial\Phi}{\partial z}\Big|_{z_n+0} - \frac{\partial\Phi}{\partial z}\Big|_{z_n-0} = -b_n\Phi_n. \quad (97)$$

Using equations (94)–(97) one can easily obtain the coefficients A_{n-1} and A_n:

$$A_{n-1} = \Phi_n \sinh^{-1}[k_D(z_n - z_{n-1})] - \Phi_{n-1} \coth[k_D(z_n - z_{n-1})], \tag{98}$$

$$A_n = \Phi_n \coth[k_D(z_n - z_{n-1})] - b_n/k_D - \Phi_{n-1} \sinh^{-1}[k_D(z_n - z_{n-1})]. \tag{99}$$

Equations (98) and (99) must be identical when $n \to n+1$. This condition gives

$$\Phi_n \left\{ \tanh\left[\frac{k_D}{2}(z_n - z_{n-1})\right] + \tanh\left[\frac{k_D}{2}(z_{n+1} - z_n)\right] - b_n/k_D \right\} = \frac{\Phi_{n-1} - \Phi_n}{\sinh[k_D(z_n - z_{n-1})]} + \frac{\Phi_{n+1} - \Phi_n}{\sinh[k_D(z_{n+1} - z_n)]}. \tag{100}$$

Thus, the solution of equation (94) takes the form

$$\Phi(z) = \frac{\Phi_n \sinh[k_D(z_{n+1} - z)] + \Phi_{n+1} \sinh[k_D(z - z_n)]}{\sinh[k_D(z_{n+1} - z_n)]}. \tag{101}$$

Under the condition specified by equation (100), the solution of equation (95) has an analogous form, which can be found from equation (101) by the replacement $n \to n-1$.

We now assume that the dust particles execute small oscillations about their equilibrium position. The dust grains are assumed to have the same potential Φ_0 (and the charge Q_0) with a uniform separation distance a. During the oscillations, distances between the grains change, and according to equation (100), the grain potential change as well. However, on the timescale of the DL wave appearance, we assume that the dust particles maintain their equilibrium potential (and the charge). Equation (101) can then be expressed in the form

$$\Phi(z) = \Phi_0 \frac{\cosh[\frac{k_D}{2}(z_{n+1} + z_n - 2z)]}{\cosh[\frac{k_D}{2}(z_{n+1} - z_n)]}. \tag{102}$$

The above expression gives the total electrostatic potential energy of the interaction for the dust grain system, namely

$$U = \sum_n Q_n \Phi(z_n) = Q_0 \Phi_0 \sum_n \frac{\cosh[\frac{k_D}{2}(z_{n+1} + z_{n-1} - 2z_n)]}{\cosh[\frac{k_D}{2}(z_{n+1} - z_{n-1})]}. \tag{103}$$

We note that in equation (103) we have excluded the interaction of the charge with its own field. The equation of motion for the nth dust grain, therefore, becomes

$$m_d \frac{\partial^2 z_n}{\partial t^2} = -\frac{\partial U}{\partial z_n}, \tag{104}$$

where U is given by equation (103). We now consider small longitudinal oscillations ($\tilde{z}_n$) of dust grains, about their equilibrium positions z_{n0}, i.e. $z_n = z_{n0} + \tilde{z}_n$, where $\tilde{z}_n \ll z_{n0}$, and derive the nonlinear equation for the DL waves. For this purpose, we need the expanded version of the potential energy U (equation (103)) and the corresponding equation of motion (equation (104)), which read

$$U = \frac{Q_0 \Phi_0}{\cosh(k_D a)} \frac{1 + \frac{k_D^2}{4}(\tilde{z}_{n+1} + \tilde{z}_{n-1} - 2\tilde{z}_n)^2 + \frac{k_D^4}{384}(\tilde{z}_{n+1} + \tilde{z}_{n-1} - 2\tilde{z}_n)^4}{1 + \frac{k_D}{2}\tanh(k_D a)(\tilde{z}_{n+1} - \tilde{z}_{n-1})}, \tag{105}$$

$$\frac{\partial^2 \tilde{z}_n}{\partial t^2} = \frac{Q_0 \Phi_0 k_D^2}{m_d \cosh(k_D a)} \frac{(\tilde{z}_{n+1} + \tilde{z}_{n-1} - 2\tilde{z}_n) + \frac{k_D^2}{48}(\tilde{z}_{n+1} + \tilde{z}_{n-1} - 2\tilde{z}_n)^3}{1 + \frac{k_D}{2}\tanh(k_D a)(\tilde{z}_{n+1} - \tilde{z}_{n-1})}. \tag{106}$$

To simplify equation (106), we will only include weak non-linearities. We will also consider the long-wavelength approximation ($k_D a \ll 1$), where the wave dispersion is small and equation (106) can be approximated by the differential equations for a continuum [27]. Thus, we introduce the Taylor expansions of $\tilde{z}_{n+1}$ and $\tilde{z}_{n-1}$ as $\tilde{z}_n + (\partial\tilde{z}/\partial z)_n a + 0.5(\partial^2\tilde{z}/\partial z^2)_n a^2 + \cdots$ and $\tilde{z}_n - (\partial\tilde{z}/\partial z)_n a + 0.5(\partial^2\tilde{z}/\partial z^2)_n a^2 + \cdots$, respectively. Inserting these expansions in equation (106), we obtain [35]

$$\frac{\partial^2\tilde{z}}{\partial t^2} - C_L^2\left[\frac{\partial^2\tilde{z}}{\partial z^2} + \frac{a^2}{12}\frac{\partial^4\tilde{z}}{\partial z^4} - \frac{k_D a}{2}\tanh(k_D a)\frac{\partial}{\partial z}\left(\frac{\partial\tilde{z}}{\partial z}\right)^2\right] = 0. \tag{107}$$

Here

$$C_L = \left[\frac{Q_0\Phi_0 k_D^2 a^2}{m_d\cosh(k_D a)}\right]^{1/2} \tag{108}$$

is the phase speed of the DL waves for $k_D a \ll 1$, where the Debye shielding around each dust particle has been neglected. Equation (107) includes the DL waves propagating in both positive and negative z directions with phase velocities close to C_L and $-C_L$, respectively. For the waves with phase velocities close to C_L, equation (107) takes the form

$$\left(\frac{\partial}{\partial t} + C_L\frac{\partial}{\partial z}\right)\tilde{z} + C_L\left[\frac{a^2}{12}\frac{\partial^3\tilde{z}}{\partial z^3} - \frac{k_D a}{2}\tanh(k_D a)\left(\frac{\partial\tilde{z}}{\partial z}\right)^2\right] = 0. \tag{109}$$

Equation (109) is now transformed to a wave-frame moving with a relative speed C_L in a new frame ($Z = z - C_L\tau$ and $\tau = t$). It is then differentiated with respect to Z, yielding the KdV equation

$$\frac{\partial u}{\partial\tau} - a_1 u\frac{\partial u}{\partial Z} + b_1\frac{\partial^3 u}{\partial Z^3} = 0 \tag{110}$$

where $u = \partial\xi/\partial Z$, $a_1 = k_D a\tanh(k_D a)$ and $b_1 = C_L a^2/12$.

The stationary solution of the KdV equation (110) is now obtained by transforming Z to $\xi = Z - u_0\tau$, where u_0 is the solitary wave speed and $\tau = T$, and imposing the appropriate boundary conditions for localized perturbations, namely $u \to 0$, $\mathrm{d}u/\mathrm{d}\xi \to 0$ and $\mathrm{d}^2u/\mathrm{d}\xi^2 \to 0$ at $\xi \to \pm\infty$. Accordingly, the stationary solution of equation (110) is of the form

$$u = -u_m\,\mathrm{sech}^2[\xi/\Delta_1], \tag{111}$$

where the amplitude u_m and width Δ_{DL} of the DL solitary waves are given by $u_m = 3u_0/a_1$ and $\Delta_1 = \sqrt{4b_1/u_0}$, respectively. As $u_0 > 0$ and $a_1 > 0$, equation (111) predicts the existence of small- but finite-amplitude DL solitary waves with $u < 0$.

Recently, Samsonov *et al* [87] have theoretically and experimentally studied the properties of DL solitary waves and compared the theoretical results with the experimental observations. The theoretical analysis of DL solitary waves presented by Samsonov *et al* [87], which is finally the same as presented by Melandsø [27], can be summarized as follows.

The longitudinal oscillations of dust grains (with a constant charge q_d) in a one-dimensional linear chain are governed by the equations of motion

$$m_d\left(\frac{\partial^2\boldsymbol{r}_j}{\partial t^2} + \nu_{dn}\frac{\partial\boldsymbol{r}_j}{\partial t}\right) = -\sum_i\frac{\partial U_{ij}}{\partial\boldsymbol{r}_j} + \boldsymbol{F}_{ext}, \tag{112}$$

$$U_{ij} = \frac{q_d^2}{|\boldsymbol{r}_i - \boldsymbol{r}_j|}\exp\left(-\frac{|\boldsymbol{r}_i - \boldsymbol{r}_j|}{\lambda_D}\right), \tag{113}$$

where $\boldsymbol{r}_j$ is the position of the jth dust particle, ν_{dn} is the collision frequency of dust particles with background neutral gas, U_{ij} is the Debye–Hückel potential and $\boldsymbol{F}_{ext}$ is the external force consisting of two components, namely a stationary confinement force and a nonstationary exciting force.

We consider a one-dimensional problem, and assume that dust particles are sufficiently strongly coupled so that they only obtain small longitudinal oscillations $x_j = x_{j0} + \tilde{x}_j$ around their equilibrium positions x_{j0}. Using the perturbation theory ($\tilde{x}_j \ll x_{j0}$) along with the long-wavelength approximation, where dust particle separation a is small in comparison with the wavelength, equation (112) can be expressed as [87]

$$\frac{\partial^2 \tilde{x}_j}{\partial t^2} + \nu_{dn}\frac{\partial \tilde{x}_j}{\partial t} = \kappa \frac{\partial}{\partial x}\left\{ \frac{C_L^2}{\kappa}\left[\frac{\partial \tilde{x}_j}{\partial x} - \frac{\Lambda}{2}\left(\frac{\partial \tilde{x}_j}{\partial x}\right)^2 \right] + \frac{\partial}{\partial x}\left[\frac{C_L^2}{\kappa}\mathcal{D}^2 \frac{\partial^2 \tilde{x}_j}{\partial x^2} \right] \right\} + \frac{F_{ext}}{m_d}, \tag{114}$$

where $C_L = C_0\sqrt{\kappa^2[G(\kappa)/\kappa]''/2}$ is the DL speed, $\kappa = a/\lambda_D$ is the lattice parameter, $C_0 = \sqrt{2q_d^2/m_d\lambda_D}$, $\Lambda = -\kappa[G(\kappa)/\kappa]'''/[G(\kappa)/\kappa]''$ is the dimensionless nonlinear coefficient and $\mathcal{D} = \sqrt{\lambda_D^2\kappa^2[G(\kappa)''/\kappa]''/[12G(\kappa)/\kappa]''}$ is the dispersion length. Here $G(\kappa) = -\ln[\exp(\kappa) - 1]$ and the prime denotes the derivative with respect to κ. It is obvious that the kinetic coefficients C_L, Λ and $\mathcal{D}$ are functions of the lattice parameter κ. These are $C_L = C_0(\sqrt{1 + \kappa + \kappa^2/2})\exp(-\kappa/2)$, $\Lambda = 3(1 + \kappa + \kappa^2/2 + \kappa^3/6)/(1 + \kappa + \kappa^2/2)$ and $\mathcal{D} = \lambda_D\kappa/\sqrt{12}$ for $\kappa \gg 1$ (nearest-neighbour approximation), whereas $C_L = C_0\sqrt{(3 - 2\ln\kappa)/2}$, $\Lambda = (11 - 6\ln\kappa)/(3 - 2\ln\kappa)$ and $\mathcal{D} = \lambda_D/\sqrt{3 - 2\ln\kappa}$ for $\kappa \ll 1$.

When the weakly inhomogeneous case is considered so that lattice parameter changes on a scale much larger than the size of the solitary waves, i.e. κ, C_L, Λ and $\mathcal{D}$, are independent of x, equation (114) can be expressed as [87]

$$\frac{\partial^2 \tilde{x}_j}{\partial t^2} + \nu_{dn}\frac{\partial \tilde{x}_j}{\partial t} = C_L^2\left[\frac{\partial^2 \tilde{x}_j}{\partial x^2} - \frac{\Lambda}{2}\frac{\partial}{\partial x}\left(\frac{\partial \tilde{x}_j}{\partial x}\right)^2 + \mathcal{D}^2\frac{\partial^4 \tilde{x}_j}{\partial x^4} \right]. \tag{115}$$

For experimental conditions the damping length ($C_L/\nu_{dn} \simeq$ 9–15 mm) is much larger than the width of the disturbance [87]. Therefore, one can omit the friction term (second term of equation (115)) and can obtain equation (26) derived by Melandsø [27], which for waves with phase velocities close to C_L can be reduced to [27]

$$\frac{\partial \tilde{x}_j}{\partial t} + C_L\frac{\partial \tilde{x}_j}{\partial x} = -\frac{\Lambda}{4}\frac{\partial}{\partial x}\left(\frac{\partial \tilde{x}_j}{\partial x}\right)^2 + \frac{C_L\mathcal{D}^2}{2}\frac{\partial^3 \tilde{x}_j}{\partial x^3}. \tag{116}$$

Transforming equation (116) to a frame X moving with the relative speed C_L with respect to the x frame ($X = x - C_L t$, $t = T$), and differentiating it with respect to Z, we obtain the well known KdV equation [27]

$$\frac{\partial v}{\partial T} - a_2 v\frac{\partial v}{\partial X} + b_2\frac{\partial^3 v}{\partial X^3} = 0 \tag{117}$$

where $v = \partial\tilde{x}_j/\partial X$, $a_2 = \Lambda/2$ and $b_2 = C_L\mathcal{D}^2/2$ are the nonlinear and the dispersion coefficients, respectively. The steady state solution is exactly similar to equation (111), i.e.

$$v = -v_m\,\mathrm{sech}^2[(X - u_0\tau)/\Delta_2], \tag{118}$$

where the amplitude v_m and the width Δ_2 are given by $3u_0/a_2$ and $\sqrt{4b_2/u_0}$, respectively. As $u_0 > 0$ and $a_2 > 0$, equation (118) predicts the existence of small- but finite-amplitude DL solitary waves with $v < 0$.

Samsonov *et al* [87] have experimentally studied the properties (amplitude and width) of the DL solitary waves and shown that the theoretical results completely agree with their experimental observations. Their experimental conditions are as follows. The experiment was performed in a capacitively coupled rf discharge. The discharge chamber had a lower disc electrode and an upper ring electrode. The upper electrode and the chamber were grounded. An rf power of 10 W (measured as forward minus reverse) was applied to the lower electrode. The working (argon) gas pressure in the chamber was 1.8 Pa. Mono-dispersive plastic microspheres (dust particles) (8.9 ± 0.1) μm in diameter were levitated in the sheath above the lower electrode forming a mono-layer hexagonal lattice. The monolayer particle cloud was about 6 cm in diameter and levitated at a height of $\simeq$9 mm above the lower electrode. The particle separation in the lattice was 650 μm at the excitation edge, 550 μm at the middle and 720 μm at the outer edge. The particles were illuminated by a horizontal thin (0.2–0.3 mm) sheet of light from a double Nd:YAG diode pumped laser (532 nm).

4. Shocks

We have studied solitary waves which arise because of the balance between the effects of nonlinearity and dispersion when the effect of dissipation is negligible in comparison with that of nonlinearity and dispersion. However, when the dissipative effect is comparable to or more dominant than the dispersive effect, one encounters shock waves. We have designed the present section to study DIA and DA shock waves [13, 65, 66, 78] and to describe their experimental observations [84].

4.1. DIA shocks

Samsonov *et al* [87] first presented an analytical model for DIA shock waves in an unmagnetized dusty plasma with a constant dust grain charge, and derived the KdV–Burgers equation, which admits shock wave solutions [13] by including an arbitrary dissipative (kinematic viscosity) term on the right-hand side of the momentum balance equation. There is an important question regarding the source/mechanism of this dissipative term. Motivated by this question, recently, we have considered an unmagnetized dusty plasma with charge fluctuating dust grains, and have proposed that dust grain charge fluctuations can give rise to this dissipative term and can be responsible for the formation of the DIA shock waves in a dusty plasma [66]. The theoretical model for DIA waves that we recently proposed in a dusty plasma with charge fluctuating dust grains can be summarized as follows.

We have seen in section 3.1.2 that the parameter η does not play any role in our analysis of the DIA solitary waves. This is because of the scaling that we have used. We now consider a situation in which we can scale the parameter η as $\eta = \epsilon^{1/2}\eta_0$ [78]. This additional scaling, the remaining stretching/scaling of other variables being as before, introduces a new term, namely $-u_0\eta_0\partial z_d^{(1)}/\partial\xi$, in the right-hand side of equation (55). Therefore, with $\eta = \epsilon^{1/2}\eta_0$, equation (55) can be rewritten as

$$-u_0\eta_0\frac{\partial z_d^{(1)}}{\partial\xi} = \beta_e\phi^{(2)} - \alpha u_\beta z_d^{(2)} + \beta_1\phi^{(1)}\frac{\partial\phi^{(1)}}{\partial\xi} - \beta_i u_1 u_i^{(2)} - u_0\beta_i u_2 n_i^{(2)}. \quad (119)$$

Replacing equation (55) by equation (119) and performing all mathematical steps as we did in

order to derive equation (58), we obtain a KdV–Burgers equation

$$\frac{\partial \phi^{(1)}}{\partial \tau} + A_c \phi^{(1)} \frac{\partial \phi^{(1)}}{\partial \xi} + B_c \frac{\partial^3 \phi^{(1)}}{\partial \xi^3} = C_c \frac{\partial^2 \phi^{(1)}}{\partial \xi^2}, \tag{120}$$

where

$$C_c = \frac{B_c v_0 \eta_0 \beta_0 (1-\mu)}{\alpha(\beta_e + 2\beta_i/u_0)}. \tag{121}$$

An exact analytical solution of equation (120) is not possible. However, we can deduce some approximate analytical solutions. Let us try to find an analytical solution which is valid for both space and laboratory dusty plasmas. We first transform the independent variables ξ to $\zeta = \xi - U_0\tau$. Under the steady state condition we then find from equation (120) a third-order ordinary differential equation for $\phi^{(1)}(\zeta) = \phi$. The latter can be integrated once, giving

$$B_c \frac{\partial^2 \phi}{\partial \zeta^2} - C_c \frac{\partial \phi}{\partial \zeta} + \frac{A_c}{2}\phi^2 - U_0 \phi = 0, \tag{122}$$

where we have imposed the appropriate boundary conditions, namely $\phi \to 0$, $\partial\phi/\partial\zeta \to 0$ and $\partial^2\phi/\partial\zeta^2 \to 0$ at $\zeta \to \infty$. For analysis, we can use a simple mechanical analogy [98] based on the fact that it has the form of an equation of motion for a pseudo-particle of mass B_c, of pseudo-time $-\zeta$ and pseudo-position ϕ in a force field with potential

$$V(\phi) = \frac{A_c}{6}\phi^3 - \frac{U_0}{2}\phi^2, \tag{123}$$

and a frictional force with coefficient C_c. The nature of the pseudo-potential $V(\phi)$ for typical space (upper plot) and laboratory (lower plot) dusty plasma parameters is depicted in figure 7. If the frictional force were absent, the quasi-particle entering from the left would go the right-hand side of the well ($\phi < 0$), reflect and return to $\phi = 0$, making a single transit. This corresponds to the DIA solitary waves defined by equation (62). However, since a frictional force is present, i.e. the particle suffers a loss of energy, it will never return to $\phi = 0$ but will oscillate about some negative value of ϕ corresponding to the minimum of $V(\phi)$. We assume that at pseudo-time $-\zeta = -\infty$, i.e. at $\zeta = \infty$, the quasi-particle is located at the coordinate origin, i.e. $\phi(\infty) = 0$, and at pseudo-time $-\zeta = \infty$, i.e. at $\zeta = -\infty$, the quasi-particle is located at a point corresponding to the minimum of $V(\phi)$, i.e. $\phi(-\infty) = 2U_0/A_c$. Thus, the solution of equation (121) describes a shock wave whose speed U_0 is related to the extreme values $\phi(\infty) = 0$ and $\phi(-\infty) = 2U_0/A_c$ by $\phi(-\infty) - \phi(\infty) = 2U_0/A_c$.

The nature of these shock structures depends on the relative values between the dispersive and dissipative coefficients B_c and C_c. If the value of C_c is very small, the energy of the particle decreases very slowly and the first few oscillations at the wavefront will be close to solitary waves as defined by equation (62). However, if the value of C_c is larger than a certain critical value, the motion of the particle will be aperiodic and we obtain a shock wave with a monotonic structure. We now determine the condition for monotonic or oscillating shock profiles by investigating the asymptotic behaviour of the solutions of equation (122) for $\zeta \to -\infty$. We first substitute $\phi(\zeta) = \phi_0 + \tilde{\phi}(\zeta)$, where $\tilde{\phi} \ll \phi_0$, into equation (122), then linearize it with respect to $\tilde{\phi}$ and obtain

$$B_c \frac{\partial^2 \tilde{\phi}}{\partial \zeta^2} - C_c \frac{\partial \tilde{\phi}}{\partial \zeta} + U_0 \tilde{\phi} = 0. \tag{124}$$

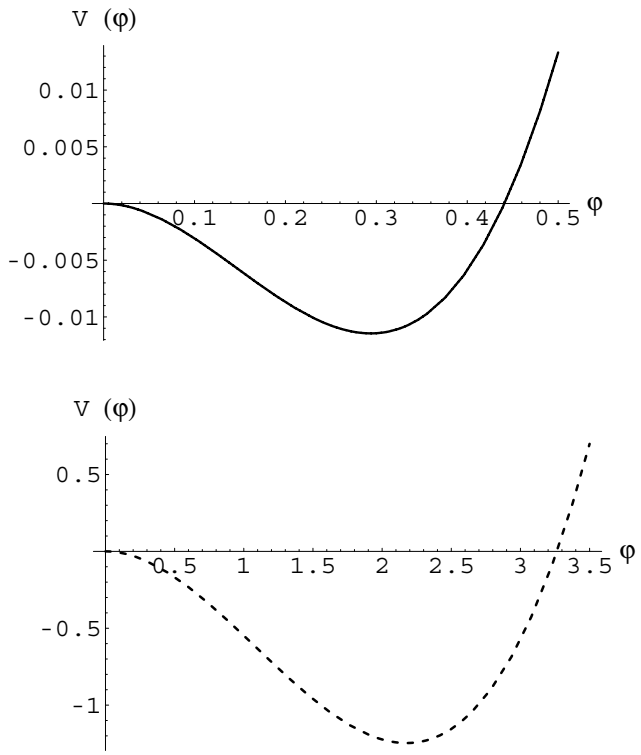

Figure 7. The behaviour of the potential $V(\phi)$ for $\mu = 0.5$. The upper plot corresponds to space dusty plasma parameters, $\alpha = 0.0288$ and $\beta = 3 \times 10^{-10}$, whereas the lower plot corresponds to laboratory dusty plasma parameters, $\alpha = 1.44$ and $\beta = 3 \times 10^{-4}$ (after [66]).

The solutions of equation (124) are proportional to $\exp(p\zeta)$, where p is given by

$$p = \frac{C_c \pm \sqrt{C_c^2 - 4B_cU_0}}{2B_c}. \tag{125}$$

This implies that the shock wave has a monotonic profile for $S_c = C_c/2\sqrt{B_cU_0} > 1$ and an oscillating profile for $S_c < 1$. We have numerically analysed S_c for space ($\alpha = 0.0288$ and $\beta = 3 \times 10^{-10}$) and laboratory ($\alpha = 1.44$ and $\beta = 3 \times 10^{-4}$) dusty plasma parameters and have found that $S_c \gg 1$ is always valid for $0 < \mu < 1$ (cf figure 8). This means that for typical space and laboratory dusty plasma parameters equation (124) (or equation (122) under steady state conditions) exhibits a monotonic shock wave solution which is given by

$$\phi^{(1)} \simeq \psi_{sh} - \psi_{sh} \tanh[(\xi - U_0\tau)/\Delta_{sh}], \tag{126}$$

where $\psi_{sh} = U_0/A_c$ and $\Delta_{sh} = 2C_c/U_0$ represent the amplitude and the width of the shock wave, respectively. We note that since $S_c \gg 1$, we have neglected the dispersive term just to avoid the complexity of the mathematics which does not affect the properties of the shock structure that may exist in our space and laboratory dusty plasmas. Since $\psi_{sh} = \psi/3$, the variation of the shock amplitude ψ_{sh} with μ for both space and laboratory dusty plasmas can be represented by the upper plot of figure 3. We have also graphically shown how the width Δ_{sh} of the shock wave varies with μ for both space ($\alpha = 0.0288$ and $\beta = 3 \times 10^{-10}$) and laboratory ($\alpha = 1.44$ and $\beta = 3 \times 10^{-4}$) dusty plasmas. This is depicted in figure 9. We note that the shock structures

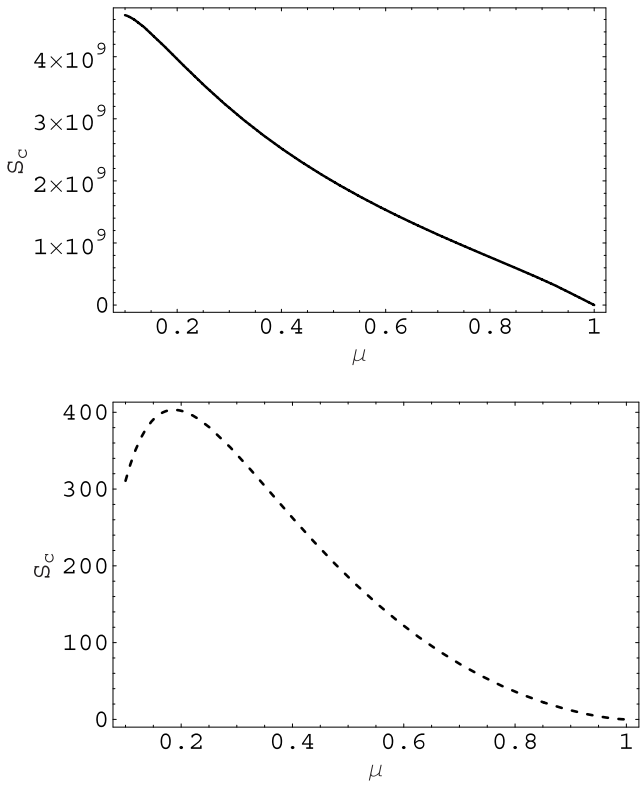

Figure 8. Variation of S_c with μ for $U_0 = 1$ and $\epsilon = 10^{-2}$. The upper plot corresponds to space dusty plasma parameters, $\alpha = 0.0288$ and $\beta = 3 \times 10^{-10}$, whereas the lower plot corresponds to laboratory dusty plasma parameters, $\alpha = 1.44$ and $\beta = 3 \times 10^{-4}$ (after [66]).

predicted by Popel *et al* [63] do not follow our shock solution (126), and look like the ion density steepening as observed by Luo *et al* [85]. However, the shock structures found in our present investigation are very close to those observed by Nakamura *et al* [84].

DIA shock waves were experimentally excited in a dusty double plasma (DP) device by Nakamura *et al* [84]. We here briefly illustrate the formation of these experimentally excited DIA shock waves by summarizing the experimental work of Nakamura *et al* [84]. The inner diameter of the dusty DP device is 40 cm and its length is 90 cm. The device is separated into a source and a target section by a fine mesh grid which is kept electrically floating. The chamber is evacuated down to 5×10^{-7} Torr with a turbo-molecular pump. The argon gas is blend into the chamber at a partial pressure of about 5×10^{-4} Torr. A dust dispersing set-up fitted at the target section consisted of a dust reservoir coupled to an ultrasonic vibrator. The dust reservoir consists of a fine stainless steel mesh (118 lines cm^{-1}) of 10 cm (width) $\times$ 16 cm (axial length) area at the bottom end and is placed horizontally closer to the anode wall. An ultrasonic vibrator is tuned at 27 kHz to vibrate the dust reservoir by using a signal generator and a power amplifier. Glass powder of average diameter 8.8 μm is used. The dust number density is easily controlled by adjusting the power of the signal applied to the vibrator and is measured from the intensity of the laser light which passes through the dust column and is collected by a photodiode array. A maximum dust density of the order of 10^5 cm^{-3} is obtained in this set-up. The plasma parameters

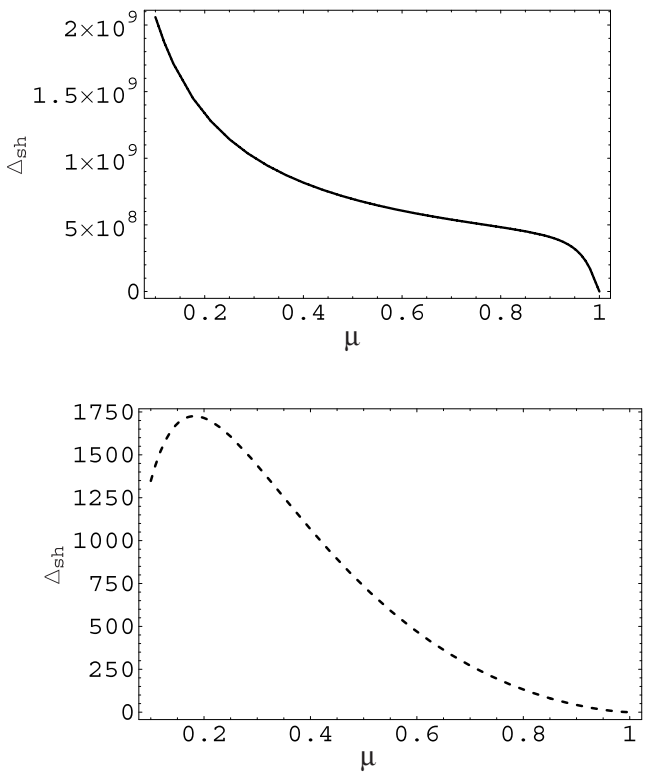

Figure 9. Variation of the shock width Δ with μ for $U_0 = 1$ and $\epsilon = 10^{-2}$. The upper plot corresponds to space dusty plasma parameters: $\alpha = 0.0288$ and $\beta = 3 \times 10^{-10}$, whereas the lower plot corresponds to laboratory dusty plasma parameters: $\alpha = 1.44$ and $\beta = 3 \times 10^{-4}$ (after [66]).

measured by a plane Langmuir probe of 6 mm diameter and a retarding potential analyser are as follows: $n_e = 10^8$–10^9 cm^{-3}, $T_e = (1$–$1.5) \times 10^4$ K, $T_i \simeq 0.1\ T_e$, $Z_d \simeq 10^5$ for $n_d < 10^3$ cm^{-3} and $Z_d \simeq 10^2$ for $n_d < 10^5$ cm^{-3}.

The shock waves are excited in the plasma by applying a ramp signal with an amplitude of 2 V and a rise time of approximately 10 μs. The Langmuir probe is biased above the plasma potential in order to detect the signal as fluctuations in the electron saturation currents. Oscillatory shock waves are first excited in the plasma without the dust and the dust density is then increased in small steps, keeping the probe fixed at 12 cm measured from the grid. The corresponding time normalized by the ion plasma period (ω_{pi}^{-1}) for the signal at 12 cm is about 150. A number of these signals are shown in figure 10, which reveals that the oscillatory wave structures behind the shock become fewer in number with increasing dust particle number density and finally completely disappears at a sufficiently high dust particle number density, leaving only the laminar shock front. The shock speed also increases with increasing dust particle number density. It is also noted that the particle density behind the shock remains constant, although the amplitude of the shock front (steepened part) seems to decrease when the dust particle number density is increased. The effect of the dust particle number density on the ion-acoustic compressional pulses has also been experimentally studied by Luo *et al* [85, 99] who observed a steepening of the ion-acoustic pulses as they propagated through a dusty plasma if the percentage of the negative charge in the plasma on the dust grains was about 75% or more.

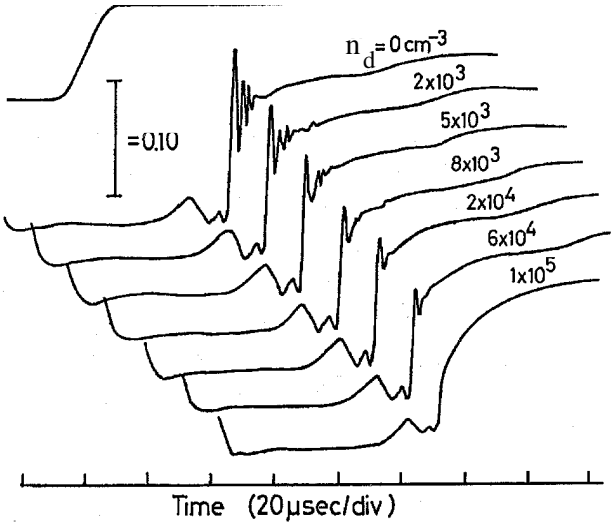

Figure 10. Variation of the plasma number density with time at a fixed probe position (12 cm) showing the transition of an oscillatory shock to a monotonic shock when the dust particle number density is increased (after [84]).

4.2. DA shocks

The nonlinear propagation of DA waves in a strongly coupled dusty plasma can be investigated by means of the generalized hydrodynamic (GH) model, namely equations (63) and (66), and

$$(1+\tau_m D_t)\left[n_d\left(D_t u_d + \nu_{dn} u_d - \frac{\partial\varphi}{\partial z}\right)\right] = \eta_d \frac{\partial^2 u_d}{\partial z^2}, \tag{127}$$

where $D_t = \partial/\partial t + u_d \partial/\partial z$, ν_{dn} is normalized by the dust plasma frequency ω_{pd}, the viscoelastic relaxation time τ_m is normalized by the dust plasma period ω_{pd}^{-1} and $\eta_d = (\tau_d/m_d n_{d0}\lambda_{Dm}^2)[\eta_b + (4/3)\zeta_b]$ is the normalized longitudinal viscosity coefficient with η_b and ζ_b being the shear and bulk transport coefficients [33].

To derive a dynamical equation for DA shock waves from our basic equations (63), (66) and (127), we employ the reductive perturbation technique. Thus, as before, we introduce the stretched coordinates $\xi = \epsilon^{1/2}(z - u_0 t)$ and $\tau = \epsilon^{3/2} t$, and use the expansion of n_d, u_d and φ, and finally derive the KdV–Burgers equation

$$A_d^{-1}\frac{\partial\varphi^{(1)}}{\partial\tau} + \varphi^{(1)}\frac{\partial\varphi^{(1)}}{\partial\xi} + \beta_d\frac{\partial^3\varphi^{(1)}}{\partial\xi^3} = \mu_d\frac{\partial^2\varphi^{(1)}}{\partial\xi^2}, \tag{128}$$

where $A_d = (v_0^3 a_d/2)(1+\nu_{dn}\tau_m/2)^{-1}$, $\beta_d = 1/a_d$, $\mu_d = \eta_{d0}/a_d v_0^3$, $a_d = (\nu_{dn}\tau_m - a_{\mu\sigma})/v_0^4$ and $a_{\mu\sigma} = 2v_0^4[1 + (3+\sigma_i\mu)\sigma_i\mu + (1+\sigma_i^2)\mu/2]/(1-\mu)^2$. Thus, for a weakly coupled or collisionless dusty plasma ($\nu_{dn}\tau_m \to 0$) we have $a_{\mu\sigma} < \nu_{dn}\tau_m$, i.e. $a_d < 0$, i.e. all coefficients (A_d, β_d and μ_d) are negative, whereas for a strongly coupled highly collisional dusty plasma satisfying $\nu_{dn}\tau_m > a_{\mu\sigma}$ we have $a_d > 0$, i.e. all coefficients (A_d, β_d and μ_d) are positive. We note that for the usual dusty plasma parameters (namely $\mu = 0.1$ and $\sigma_i = 1$) we have $a_{\mu\delta} \simeq 2.0$. This means that for $T_i \leq T_e$ and $n_{e0} \leq 0.1\, n_{i0}$ all coefficients (A_d, β_d and μ_d) can be positive if $\nu_{dn}\tau_m \geq 2$.

We now find the shock solutions of the KdV–Burgers equation (128) which, after transformation of the space variable ξ–$\zeta = \xi - U_0\tau$, where U_0 is the normalized velocity of the shock waves, can be integrated once, yielding

$$\beta_d \frac{d^2\varphi^{(1)}}{d\zeta^2} - \mu_d \frac{d\varphi^{(1)}}{d\zeta} + \frac{1}{2}[\varphi^{(1)}]^2 - \frac{U_0}{A_d}\varphi^{(1)} = 0, \tag{129}$$

where we have used the steady state condition and have imposed the appropriate boundary conditions, namely $\varphi^{(1)} \to 0$, $d\varphi^{(1)}/d\zeta \to 0$ and $d^2\varphi^{(1)}/d\zeta^2 \to 0$ at $\zeta \to \infty$. We can now easily show [98, 100] that equation (129) describes a shock wave whose speed U_0 is related to the extreme values $\varphi^{(1)}(-\infty) - \varphi^{(1)}(\infty) = Y$ by $U_0/A_d = Y/2$. Thus, in the rest frame the normalized speed of the shock waves is $(1 + A_d Y/2)$. The nature of these shock waves depends on the relative values of the dispersive and dissipative parameters β_d and μ_d.

We first consider a situation where the dissipative term is dominant over the dispersive term, i.e. we can express equation (129) as

$$\left(\varphi^{(1)} - \frac{U_0}{A_d}\right)\frac{d\varphi^{(1)}}{d\zeta} = \mu_d \frac{d^2\varphi^{(1)}}{d\zeta^2}. \tag{130}$$

Using the condition that y is bounded as $\zeta \to \pm\infty$, equation (130) can be integrated to obtain [98]

$$\varphi^{(1)} = \frac{U_0}{A_d}\left[1 - \tanh\left(\frac{U_0}{2\mu_d}(\xi - U_0\tau)\right)\right]. \tag{131}$$

Equation (131) represents a monotonic shock solution with the shock speed U_0, the shock height U_0/A_d and the shock thickness $2\mu_d/U_0$. The shock solution appears because of the dissipative term, which is proportional to the viscosity coefficient.

Now, we discuss the combined effects of dissipation (β_d) and dispersion (μ_d). When μ_d is extremely small, the shock waves will have an oscillatory profile in which the first few oscillations at the wavefront will be close to solitons moving with the speed U_0 [98]. If μ_d is increased and it is larger than a critical value μ_{dc}, the shock wave will have a monotonic behaviour. To determine the value of the dissipation coefficient μ_d corresponding to monotonic or oscillating shock profiles, we investigate the asymptotic behaviour of the solution of equation (129) for $\zeta \to -\infty$. We first substitute $\varphi^{(1)}(\zeta) = y_0 + y_1(\zeta)$, where $y_1 \ll y_0$, into equation (129) and then linearize it with respect to y_1 in order to obtain

$$\beta_d \frac{\partial^2 y_1}{\partial\zeta^2} - \mu_d \frac{\partial y_1}{\partial\zeta} + \frac{U_0}{A_d} y_1 = 0. \tag{132}$$

The solution of equation (132) is proportional to $\exp(p_s x)$, where p_s is

$$p_s = \frac{\mu_d}{2\beta_d} \pm \left(\frac{\mu_d^2}{4\beta_d^2} - \frac{U_0}{A_d\beta_d}\right)^{1/2}. \tag{133}$$

It turns out that the shock wave has a monotonic profile for $\mu_d > \mu_{dc}$ and an oscillatory profile for $\mu_d < \mu_{dc}$, where $\mu_{dc} = (4\beta_d U_0/A_d)^{1/2}$.

5. Vortices

Coherent vortices appear in two-dimensional fluids and magnetized plasmas. In a simplest possible scenario, the vortex dynamics is governed by the Navier–Stokes (NS) equation which admits a monopolar vortex. However, in a magnetized dusty plasma we have the possibility of

vortices comprising a dipolar [80], a tripolar and a chain [81]. Here the vortices are associated with nonlinear dispersive waves that possess, at least, a two-dimensional character. When the velocity of the fluid (or plasma particle) motion associated with the dispersive waves becomes locally larger than the wave phase velocity because of the nonlinear effects, one encounters a curving of the wavefront which leads to the formation of a two-dimensional travelling vortex structure.

5.1. Electrostatic vortices

We know that the low-frequency (in comparison with the ion gyrofrequency) SV mode [46] involves two-dimensional electron and ion motions in a nonuniform dusty magnetoplasma containing stationary dust grains. We now discuss possible vortex solutions involving nonlinear SV modes. In the presence of low-frequency (namely $\omega_{cd}, \omega_{pd} \ll |\mathrm{d}/\mathrm{d}t| \ll \omega_{ci}$, where ω_{ci} (ω_{cd}) is the ion (dust) gyrofrequency) electrostatic waves, the electron and ion velocities in our collisionless cold dusty plasma are [13]

$$\boldsymbol{v}_e \approx \frac{c}{B_0}\hat{\boldsymbol{z}} \times \nabla\phi, \tag{134}$$

$$\boldsymbol{v}_i \approx \frac{c}{B_0}\hat{\boldsymbol{z}} \times \nabla\phi - \frac{c}{B_0\omega_{ci}}\left(\frac{\partial}{\partial t} + \frac{c}{B_0}\hat{\boldsymbol{z}} \times \nabla\phi \cdot \nabla\right)\nabla_\perp\phi, \tag{135}$$

where the dynamics of the electrons and ions parallel to the external magnetic field $\hat{\boldsymbol{z}}B_0$ has been neglected. The last term on the right-hand side of equation (135) represents the nonlinear ion polarization drift [101, 102]. It comes from the advection term $(\boldsymbol{v}_i \cdot \nabla \boldsymbol{v}_i)$ in the ion momentum equation. Substituting equations (134) and (135) into the electron and ion continuity equations, letting $n_j = n_{j0} + n_{j1}$, where $n_{j1} \ll n_{j0}$, and subtracting the ion continuity equation from that of the electrons, we obtain after using $n_{e1} = n_{i1}$

$$\left(\frac{\partial}{\partial t} + \frac{c}{B_0}\hat{\boldsymbol{z}} \times \nabla\phi \cdot \nabla\right)\nabla_\perp^2\phi + u_{sv}\frac{\partial\phi}{\partial y} = 0, \tag{136}$$

which governs the nonlinear dynamics of the SV modes. Here we have denoted $u_{sv} = \omega_{ci}/k_n$. In a uniform magnetoplasma, equation (136) takes the form

$$\left(\frac{\partial}{\partial t} + \frac{c}{B_0}\hat{\boldsymbol{z}} \times \nabla\phi \cdot \nabla\right)\nabla_\perp^2\phi = 0, \tag{137}$$

which is the NS equation governing the dynamics of two-dimensional convective cells in a collisionless plasma. Equation (137) admits dual cascading and a monopolar vortex [102]. The presence of the inhomogeneous term (the third term) on the left-hand side of equation (136) provides the possibility of a stationary dipolar vortex structure, as discussed below.

We seek a solution of the generalized NS equation (136) in the stationary frame $\xi = y - ut$, where u is the translational speed of the vortex. Thus equation (136) takes the form

$$u\frac{\partial}{\partial\xi}\nabla_\perp^2\phi - u_{sv}\frac{\partial\phi}{\partial\xi} - \frac{c}{B_0}J(\phi, \nabla_\perp^2\phi) = 0, \tag{138}$$

where the Jacobian is denoted by

$$J(\phi, \nabla_\perp^2\phi) = \left(\frac{\partial\phi}{\partial x}\frac{\partial}{\partial\xi} - \frac{\partial\phi}{\partial\xi}\frac{\partial}{\partial x}\right)\nabla_\perp^2\phi, \tag{139}$$

with $\nabla_\perp^2\phi = (\partial^2\phi/\partial x^2) + (\partial^2\phi/\partial\xi^2)$. Equation (138) is satisfied by the ansatz

$$\nabla_\perp^2\phi = C_1\phi + C_2 x \tag{140}$$

provided that the constants C_1 and C_2 are related by $uC_1 - u_{sv} - (c/B_0)C_2 = 0$. The double-vortex solution of equation (140) can be constructed following standard methods [103]. Accordingly, we divide the (r, θ) plane into an outer region $r > R_v$ and an inner region $r < R_v$, where $r = (x^2 + \xi^2)^{1/2}$ and $\theta = \arctan(\xi/x)$ are the polar coordinates and R_v corresponds to the vortex radius. For localized solutions we must have $C_2 = 0$ in the outer region so that $C_1^o = u_{sv}/u \equiv k_0^2$. The outer region solution is

$$\phi^o(r, \theta) = \phi_0 K_1(k_0 r)\cos\theta, \tag{141}$$

where ϕ_0 is a constant and K_1 is the modified Bessel function of the first kind. Thus a well behaved outer solution is possible for $k_0^2 > 0$, which is satisfied for $u_{sv} > 0$. The inner region solution is

$$\phi^i = \left[\phi_i J_1(k_i r) + \frac{C_v}{k_i^2} r\right]\cos\theta, \tag{142}$$

where ϕ_i, $k_i = -C_1^i$ and $C_v = uB_0(k_0^2 + k_i^2)/c$ are constants and J_1 is the Bessel function of the first order. The superscripts o and i stand for the quantities in the outer and inner regions, respectively. The constants ϕ_0 and ϕ_i are determined from the continuity of ϕ and $\nabla_\perp^2\phi$ at the vortex interface $r = R_v$. One finds that

$$\phi_0 = \frac{R_v C_v}{(k_0^2 + k_i^2)K_1(k_0 R_v)}, \tag{143}$$

$$\phi_i = -\frac{k_0^2 R_v C_v}{k_i^2(k_0^2 + k_i^2)J_1(k_i R_v)}. \tag{144}$$

For a given value of $k_0 > 0$, the value of k_i is determined from

$$\frac{J_2(k_i R_v)}{J_1(k_i R_v)} = -\frac{k_i K_2(k_0 R_v)}{k_0 K_1(k_0 R_v)}, \tag{145}$$

which comes from the matching of $\nabla_\perp\phi$ at $r = R_v$. Here J_2 and K_2 are the Bessel and modified Bessel functions of the second order.

5.2. *Electromagnetic vortices*

We now discuss electromagnetic vortices [82] that involve nonlinear low-frequency (in comparison with the ion gyrofrequency), long-wavelength (in comparison with the ion gyroradius) electromagnetic waves in a nonuniform dusty magnetoplasma containing a density inhomogeneity along the x-axis. The dust component is considered to be immobile. In the electromagnetic fields, the electron and ion fluid velocities in a warm dusty plasma are [13]

$$\boldsymbol{v}_e \approx \frac{c}{B_0}\hat{\boldsymbol{z}} \times \nabla\phi - \frac{ck_B T_e}{eB_0 n_e}\hat{\boldsymbol{z}} \times \boldsymbol{\nabla} n_e + v_{ez}\left(\hat{\boldsymbol{z}} + \frac{\nabla A_z \times \hat{\boldsymbol{z}}}{B_0}\right), \tag{146}$$

$$\boldsymbol{v}_i \approx \frac{c}{B_0}\hat{\boldsymbol{z}} \times \nabla\phi + \frac{ck_B T_i}{eB_0 n_i}\hat{\boldsymbol{z}} \times \boldsymbol{\nabla} n_i - \frac{c}{B_0\omega_{ci}}\left(\frac{\partial}{\partial t} + \boldsymbol{v}_i \cdot \boldsymbol{\nabla}\right)\nabla_\perp\phi, \tag{147}$$

where the parallel component of the electron fluid velocity is given by

$$v_{ez} \approx \frac{c}{4\pi n_e e}\boldsymbol{\nabla}_\perp^2 A_z, \tag{148}$$

and we have ignored the ion motion parallel to $\hat{z}$ as well as neglecting the compressional magnetic field perturbation. Thus the DIA and magnetosonic waves are decoupled in our low-β ($\beta \ll 1$) dusty plasma system.

Substituting equation (146) into the electron continuity equation, letting $n_j = n_{j0}(x) + n_{j1}$, where $n_{j1} \ll n_{j0}$ and using equation (148) we obtain

$$\frac{\mathrm{d}n_{e1}}{\mathrm{d}t} - \frac{c}{B_0}\frac{\partial n_{e0}}{\partial x}\frac{\partial \phi}{\partial y} + \frac{c}{4\pi e}\frac{\mathrm{d}\nabla_\perp^2 A_z}{\mathrm{d}z} = 0, \tag{149}$$

where $\mathrm{d}/\mathrm{d}t = (\partial/\partial t) + (c/B_0)\hat{z} \times \nabla\phi \cdot \nabla$ and $\mathrm{d}/\mathrm{d}z = (\partial/\partial z) + B_0^{-1}\nabla A_z \times \hat{z} \cdot \nabla$. We have assumed $v_{EB} \cdot \nabla \gg v_{ez}\partial/\partial z$, which implies that $(\omega_{pe}^2/\omega_{ce})|\hat{z} \times \nabla\phi \cdot \nabla| \gg c\partial_z \nabla_\perp^2 A_z$. On the other hand, substitution of the ion fluid velocity into the ion continuity equation yields

$$\frac{\mathrm{d}n_{i1}}{\mathrm{d}t} - \frac{c}{B_0}\frac{\partial n_{i0}}{\partial x}\frac{\partial \phi}{\partial y} - \frac{cn_{i0}}{B_0\omega_{ci}}\left(\frac{\mathrm{d}}{\mathrm{d}t} + u_{i*}\frac{\partial}{\partial y}\right)\nabla_\perp^2\phi - \frac{c^2 k_B T_i}{eB_0^2\omega_{ci}}\nabla_\perp \cdot [(\hat{z} \times \nabla n_{i1}) \cdot \nabla\nabla_\perp\phi] = 0, \tag{150}$$

where $u_{i*} = (ck_B T_i/eB_0 n_{i0})\partial n_{i0}/\partial x$ is the unperturbed ion diamagnetic drift speed. Subtracting equation (150) from equation (149) and assuming $n_{i1} = n_{e1}$, we obtain the modified ion vorticity equation

$$\left(\frac{\mathrm{d}}{\mathrm{d}t} + u_{i*}\partial_y\right)\nabla_\perp^2\phi + \frac{V_A^2}{c}\frac{\mathrm{d}\nabla_\perp^2 A_z}{\mathrm{d}z} + u_{sv}\frac{\partial\phi}{\partial y} + \frac{ck_B T_i}{eB_0 n_{i0}}\nabla_\perp \cdot [(\hat{z} \times \nabla n_{e1}) \cdot \nabla\nabla_\perp\phi] = 0. \tag{151}$$

By using equations (146) and (148), the parallel component of the electron momentum equation can be written as

$$\left(\frac{\partial}{\partial t} + u_{e*}\frac{\partial}{\partial y}\right)A_z - \lambda_e^2\frac{\mathrm{d}\nabla_\perp^2 A_z}{\mathrm{d}t} + c\frac{\mathrm{d}\phi}{\mathrm{d}z} - \frac{ck_B T_e}{en_{e0}}\frac{\mathrm{d}n_{e1}}{\mathrm{d}z} = 0, \tag{152}$$

where $u_{e*} = -(ck_B T_e/eB_0 n_{e0})\partial n_{e0}/\partial x$ is the unperturbed electron diamagnetic drift speed.

Let us now seek stationary solutions [82] of the nonlinear equations (149), (151) and (152) by assuming that all the field variables depend on x and $\eta = y + \alpha z - ut$, where α represents the angle between the wavefront normal and the (x, y) plane. Two cases are considered.

5.2.1. Warm plasma. In the stationary η-frame, equation (152) for $\lambda_e^2|\nabla_\perp^2| \ll 1$ can be written as

$$\hat{D}_A\left(\phi - \frac{k_B T_e}{en_{e0}}n_{e1} - \frac{u - u_{e*}}{\alpha c}A_z\right) = 0, \tag{153}$$

where $\hat{D}_A = (\partial/\partial\eta) + (1/\alpha B_0)[(\partial A_z/\partial\eta)(\partial/\partial x) - (\partial A_z/\partial x)(\partial/\partial\eta)]$. A solution of equation (153) is [104]

$$n_{e1} = \frac{n_{e0}e}{k_B T_e}\phi - \frac{(u - u_{e*})n_{e0}e}{\alpha c k_B T_e}A_z. \tag{154}$$

Writing equation (149) in the stationary frame and making use of equation (154) it can be put in the form

$$\hat{D}_A\left[\lambda_{De}^2\nabla_\perp^2 A_z + \frac{u(u - u_{e*})}{\alpha^2 c^2}A_z - \frac{u - u_{e*}}{\alpha c}\phi\right] = 0. \tag{155}$$

A solution of equation (165) is

$$\lambda_{De}^2 \nabla_\perp^2 A_z + \frac{u(u-u_{e*})}{\alpha^2 c^2} A_z - \frac{u-u_{e*}}{\alpha c}\phi = 0. \tag{156}$$

The modified ion vorticity equation (151) for cold ions can be expressed as

$$\hat{D}_\phi(\nabla_\perp^2 \phi - k_0^2 \phi) - \frac{V_A^2 \alpha}{cu}\hat{D}_A \nabla_\perp^2 A_z = 0, \tag{157}$$

where $\hat{D}_\phi = (\partial/\partial\eta) - (c/uB_0)[(\partial\phi/\partial x)(\partial/\partial\eta) - (\partial\phi/\partial\eta)(\partial/\partial x)]$. Combining equations (156) and (157), we obtain

$$\hat{D}_\phi\left(\nabla_\perp^2\phi + \frac{p}{\rho_s^2}\phi + \frac{u-u_{e*}}{\alpha c\rho_s^2}A_z\right) = 0, \tag{158}$$

where $p = (C_S/u)[K_d\rho_s + (u_{e*}-u)/C_S]$. A typical solution of equation (158) is

$$\nabla_\perp^2\phi + \frac{p}{\rho_s^2}\phi + \frac{u-u_{e*}}{\alpha c\rho_s^2}A_z = C_3\left(\phi - \frac{uB_0}{c}x\right), \tag{159}$$

where C_3 is an integration constant. Eliminating A_z from equations (156) and (159), we obtain a fourth-order inhomogeneous differential equation [82]

$$\nabla^4\phi + F_1\nabla_\perp^2\phi + F_2\phi + C_3\frac{u^2(u-u_{e*})B_0}{\alpha^2 c^3\lambda_{De}^2}x = 0, \tag{160}$$

where $F_1 = p/\rho_s^2 - C_3 + u(u-u_{e*})/\alpha^2c^2\lambda_{De}^2$ and $F_2 = (u-u_{e*})^2/\alpha^2c^2\lambda_{De}^2\rho_s^2 + (p-C_3\rho_s^2)u(u-u_{e*})/\alpha^2c^2\lambda_{De}^2\rho_s^2$. We note that in the absence of charged dust we have $u_{sv} = 0$ and $F_2 = 0$ in the outer region when $C_3 = 0$. In such a situation, the outer region solution of equation (160) would have a long tail (decaying as $1/r$) for $(u-u_{e*})(\alpha^2V_A^2 - u^2) > 0$ [104]. On the other hand, inclusion of a small fraction of dust grains would make F_2 finite in the outer region. Here we have the possibility of well behaved solutions. In fact, equation (160) admits spatially bounded dipolar vortex solutions. In the outer region ($r > R_v$), we set $C_3 = 0$ and obtain the solution of equation (160) as [104]

$$\phi^o = [Q_1K_1(s_1r) + Q_2K_1(s_2r)]\cos\theta, \tag{161}$$

where Q_1 and Q_2 are constants and $s_{1,2}^2 = -[-\alpha_1 \pm (\alpha_1^2 - 4\alpha_2)^{1/2}/2]$ for $\alpha_1 < 0$ and $\alpha_1^2 > 4\alpha_2 > 0$. Here, $\alpha_1 = (p/\rho_s^2) + u(u-u_{e*})/\alpha^2c^2\lambda_{De}^2$ and $\alpha_2 = [(u-u_{e*})^2 + u(u-u_{e*})p]/\alpha^2c^2\lambda_{De}^2\rho_s^2$. In the inner region ($r < R_v$), the solution reads

$$\phi^i = \left[Q_3J_1(s_3r) + Q_4I_1(s_4r) - \frac{C_3^i}{\lambda_{De}^2}\frac{u^2(u-u_{e*})B_0}{\alpha^2c^3F_2^i}r\right]\cos\theta, \tag{162}$$

where Q_3, Q_4, C_3^i and F_2^i are constants. We have defined $s_{3,4} = [(F_1^{i2} - 4F_2^i)^{1/2} \pm F_1^i]/2$ for $F_2^i < 0$. Thus, the presence of charged dust grains is responsible for the complete localization of the vortex solutions both in the outer as well as in the inner regions of the vortex core.

5.2.2. Cold plasma. We now present the double-vortex solution of equations (151) and (152) in the cold-plasma approximation. Hence we set $T_j = 0$ and write equation (151) in the form of equation (157), while equation (152) in the stationary frame can be expressed as

$$\hat{D}_\phi\left[\left(1-\lambda_e^2\nabla_\perp^2\right)A_z - \frac{\alpha c}{u}\phi\right] = 0. \tag{163}$$

It is easy to verify that equation (163) is satisfied by

$$(1-\lambda_e^2\nabla_\perp^2)A_z - \frac{\alpha c}{u}\phi = 0. \tag{164}$$

By using equation (164) one can eliminate $\nabla_\perp^2 A_z$ from equation (157), obtaining

$$\hat{D}_\phi\left[\nabla_\perp^2\phi - k_0^2\phi + \frac{\alpha^2 V_A^2}{c^2\lambda_e^2}\phi - \frac{\alpha V_A^2}{uc\lambda_e^2}A_z\right] = 0. \tag{165}$$

A typical solution of equation (165) is

$$\nabla_\perp^2\phi + \beta_1\phi - \beta_2 A_z = C_4\left(\phi - \frac{uB_0}{c}x\right), \tag{166}$$

where $\beta_1 = (\alpha^2 V_A^2/u^2\lambda_e^2) - k_0^2$, $\beta_2 = \alpha V_A^2/uc\lambda_e^2$ and C_4 is an integration constant. Eliminating A_z from equations (164) and (166) we obtain

$$\nabla_\perp^4\phi + G_1\nabla_\perp^2\phi + G_2\phi - \frac{C_4 uB_0}{\lambda_e^2 c}x = 0, \tag{167}$$

where $G_1 = \lambda_e^{-2}[(\alpha^2 V_A^2/c^2) - 1] - k_0^2 - C_4$ and $G_2 = (C_4 - k_0^2)/\lambda_e^2$. Equation (167) is similar to equation (160) and its bounded solutions (similar to equations (161) and (162)) exist provided that $u^2(1 + k_0^2\lambda_e^2) > \alpha^2 V_A^2$ and $u_{sv} > 0$. In the absence of the dust, we have $G_2 = 0$ in the outer region ($C_4 = 0$), and the outer region solution of equation (167) for the dust-free case also has a long tail. The various constants are contained in [104].

6. Discussion

In this paper, we have presented theoretical and experimental studies of the DIA, DA and DL solitary waves, DIA and DA shock waves and electrostatic and electromagnetic vortices in dusty plasma. The results which have been obtained from these studies can be summarized as follows.

The DIA solitary waves with a positive (negative) potential can exist for $\mu > (<)\ 1/3$. To examine how the ion fluid temperature (σ_i) modifies the properties of the arbitrary amplitude DIA solitary waves, we found that as we increase σ_i,

(i) we need a higher value of the cortical Mach number (corresponding to a lower value of μ) in order to have DIA solitary waves with negative potential, and

(ii) the amplitude of both positive and negative solitary waves decreases, but their width increases.

To examine the effect of a non-planar geometry on DIA solitary waves, we found that the term $(\nu/2\tau)\phi^{(1)}$ in equation (35) is due to a non-planar (cylindrical or spherical) geometry. The numerical solutions of equation (35) (cf figures 1 and 2) reveal that for a large value of τ (e.g. $\tau = -9$) the spherical and cylindrical solitary waves are similar to one-dimensional solitary waves. This is because, for a large value of τ, the term $(\nu/2\tau)\phi^{(1)}$, which is due to the effect

of the cylindrical or spherical geometry, is no longer dominant. However, as the value of τ decreases, the term $(\nu/2\tau)\phi^{(1)}$ becomes dominant and both spherical and cylindrical solitary waves differ from one-dimensional solitary waves. It is found that as the value of τ decreases, the amplitude of these localized pulses increases. We also note that the amplitude of cylindrical solitary waves is larger than that of the one-dimensional solitary waves, but smaller than that of the spherical ones. We have shown that the effects of dust grain charge fluctuations modify the properties of the DIA solitary waves. It has been found that the effects of dust grain charge fluctuations reduce the speed of the DIA solitary waves. The characteristics of these DIA solitary waves in the space dusty plasma condition are found to be different from those in the laboratory dusty plasma condition. It is seen that for the parameters corresponding to space dusty plasma situations [6, 13], as we increase μ, both the amplitude and the width of the DIA solitary waves remain constant for $\mu < 0.5$, but increase very rapidly for $\mu > 0.5$. On the other hand, for laboratory dusty plasma parameters [26, 34], as we increase μ, the amplitude increases, but the width decreases.

The dusty plasma containing mobile dust particles and Boltzmann electrons and ions can support DA solitary waves with a negative potential only, corresponding to a hump in the dust number density. We found that as we increase the dust fluid temperature, the amplitude of DA solitary waves decreases, but their width increases. We have shown that due to the effect of the trapped ion distribution, a dusty plasma admits a modified KdV equation, exhibiting a stronger nonlinearity, smaller width and larger propagation speed. When we consider a nonplanar geometry (cylindrical or spherical), we find that a dusty plasma admits a modified KdV equation containing $(\nu/2\tau)\varphi^{(1)}$. This extra term is due to the effect of cylindrical ($\nu = 1$) or spherical ($\nu = 2$) geometry. It is seen that as the value of τ decreases, the amplitude of these localized pulses increases. Furthermore, the cylindrical solitary waves travel more quickly than the one-dimensional solitary waves but more slowly than the spherical ones, and the amplitude of cylindrical solitary waves is larger than that of the one-dimensional solitary waves, but slightly smaller than that of the spherical ones.

We have studied the properties of DL solitary waves by constructing a nonlinear evolution equation, which admits a solitary wave solution. We have shown that small- but finite-amplitude DL solitary waves exist with $\partial\xi/\partial Z < 0$.

The dust grain charge fluctuations are responsible for the formation of DIA shock waves in both space and laboratory dusty plasmas. The shock wave amplitude is one-third of the solitary wave amplitude, but their dependences on dusty plasma parameters are exactly the same. Furthermore, the shock width decreases with μ (when $1 > \mu > 0.2$) for both space and laboratory dusty plasma parameters. However, for $0 < \mu < 0.2$ as we increase μ, the shock width increases for laboratory dusty plasma conditions, but decreases for space dusty plasma conditions.

A strongly coupled (correlated) dusty plasma may support DA shock waves instead of DA solitary structures due to the dissipation effect μ_d. When μ_d is extremely small, shock waves will have an oscillatory profile in which the first few oscillations will be close to solitary structures. If μ_d is increased and it is larger than a critical value μ_{dc}, shock waves will have a monotonic behaviour.

In an external magnetic field, dusty plasmas support a great variety of obliquely propagating electrostatic and electromagnetic waves. Inclusion of density inhomogeneities introduces such novel modes as the SV mode. Here, we can have multi-dimensional solitary and shock waves. For illustrative purposes, we have studied the properties of electrostatic and electromagnetic

vortices that may form in a nonuniform dusty magnetoplasma. We have shown that the nonlinear SV modes that involve two-dimensional electron and ion motions in a nonuniform dusty magnetoplasma containing stationary dust grains form a stationary dipolar vortex structure. The nonlinear propagation of low-frequency (in comparison with the ion gyrofrequency, long-wavelength (in comparison with the ion gyroradius) electromagnetic waves in non-uniform dusty magnetoplasma is also found to form vortex structures in which the presence of charged dust grains is responsible for the complete localization of vortex solutions in the centre as well as the inner regions of the vortex core.

Acknowledgments

AAM gratefully acknowledges the financial support of the Alexander von Humboldt-Stiftung (Bonn, Germany). This work was partially supported by the European Commission (Brussels) through contract no HPRN-CT-2000-00140 for carrying out the task of the Human Potential and Training Network entitled 'Complex plasmas: the science of laboratory colloidal plasmas and mesospheric charged aerosols' and by the Deutsche Forschungsgemeinschaft (Bonn) through the Sonderforschungsbereich 591.

References

[1] Goertz C K 1989 *Rev. Geophys.* **27** 271
[2] Mendis D A 1991 *Astrophys. Space Sci.* **176** 163
[3] Mendis D A 1997 *Advances in Dusty Plasmas* ed P K Shukla, D A Mendis and T Desai (Singapore: World Scientific) pp 3–19
[4] Mendis D A and Horanyi M 1991 *Cometary Plasma Processes* ed A J Johnston (Washington, DC: Geophys) p 17
[5] de Angelis U 1992 *Phys. Scr.* **45** 465
[6] Mendis D A and Rosenberg M 1994 *Annu. Rev. Astron. Astrophys.* **32** 419
[7] Shukla P K 1996 *The Physics of Dusty Plasmas* (Singapore: World Scientific) pp 107-21
[8] Verheest F 1996 *Space Sci. Rev.* **77** 267
[9] Nakano T. 1998 *Astrophys. J.* **494** 587
[10] Zweibel E 1999 *Phys. Plasmas* **6** 1725
[11] Verheest F 2000 *Waves in Dusty Space Plasmas* (Dordrecht: Kluwer)
[12] Shukla P K 2001 *Phys. Plasmas* **8** 1791
[13] Shukla P K and Mamun A A 2002 *Introduction to Dusty Plasma Physics* (Bristol: Institute of Physics Publishing)
[14] Mendis D A 2002 *Plasma Sources Sci. Technol.* **11** A219
[15] Shukla P K 2002 *Dust Plasma Interaction in Space* (New York: Nova)
[16] Winter J 1998 *Plasma Phys. Control. Fusion* **40** 1201
[17] Bouchoule A 1999 *Dusty Plasmas: Physics, Chemistry and Technical Impacts in Plasma Processing* ed A Bouchoule (New York: Wiley) pp 305–96
[18] Hollenstein C 2000 *Plasma Phys. Control. Fusion* **42** R93
[19] Rao N N, Shukla P K and Yu M Y 1990 *Planet. Space Sci.* **38** 543
[20] Shukla P K and Silin V P 1992 *Phys. Scr.* **45** 508
[21] Verheest F 1992 *Planet. Space Sci.* **40** 1
[22] Varma R K, Shukla P K and Krishan V 1993 *Phys. Rev.* E **47** 3612
[23] Melandsø F, Aslaksen T and Havnes O 1993 *Planet. Space Sci.* **41** 321

[24] Winske D, Gary S P, Jones M E, Rosenberg M, Mendis D A and Chow V W 1995 *Geophys. Res. Lett.* **22** 2069
[25] Barkan A, Merlino R L and D'Angelo N 1995 *Phys. Plasmas* **2** 3563
[26] Barkan A, D'Angelo N and Merlino R L 1996 *Planet. Space Sci.* **44** 239
[27] Melandsø F 1996 *Phys. Plasmas* **3** 3890
[28] Rosenberg M 1996 *J. Vac. Sci. Technol.* A **14** 631
[29] Salimullah M 1996 *Phys. Lett.* A **215** 296
[30] Rosenberg M and Kalman G 1997 *Phys. Rev.* E **56** 7166
[31] Homann A, Melzer A, Peters S and Piel A 1997 *Phys. Rev.* E **56** 7138
[32] Morfill G E, Thomas H M and Zuzic M 1997 *Advances in Dusty Plasmas* ed P K Shukla, D A Mendis and T Desai (Singapore: World Scientific) pp 99–142
[33] Kaw P K and Sen A 1998 *Phys. Plasmas* **5** 3552
[34] Merlino R L, Barkan A, Thompson C and D'Angelo N 1998 *Phys. Plasmas* **5** 1607
[35] Farokhi B, Shukla P K, Tsintsadze N L and Tskhakaya D D 1999 *Phys. Lett.* A **264** 318
[36] Thompson C, Barkan A, Merlino R L and D'Angelo N 1999 *IEEE Trans. Plasma Sci.* **27** 146
[37] Luo Q Z, D'Angelo N and Merlino R L 2001 *Phys. Plasmas* **8** 31
[38] Hill J R and Mendis D A 1981 *Moon Planets* **24** 431
[39] Smith B A *et al* 1981 *Science* **212** 163
[40] Smith B A *et al* 1982 *Science* **215** 504
[41] Horányi M and Goertz C K 1990 *Astrophys. J.* **361** 105
[42] Bliokh P V and Yaroshenko V V 1985 *Sov. Astron.* **29** 330
[43] de Angelis U, Formisano V and Giordano M 1988 *J. Plasma Phys.* **40** 399
[44] Shukla P K and Stenflo L 1992 *Astrophys. Space Sci.* **190** 23
[45] Shukla P K, Yu M Y and Bharuthram R 1993 *J. Geophys. Res.* **96** 21343
[46] Shukla P K and Varma R K 1993 *Phys. Fluids* B **5** 236
[47] Shukla P K 1992 *Phys. Scr.* **45** 504
[48] Shukla P K and Rahman H U 1996 *Phys. Plasmas* **3** 430
[49] Birk G T, Kopp A and Shukla P K 1996 *Phys. Plasmas* **3** 3564
[50] Ikezi H 1986 *Phys. Fluids* **29** 1764
[51] Chu J H and Lin I 1994 *Phys. Rev. Lett.* **72** 4009
[52] Thomas H, Morfill G E, Demmel V, Goree J, Feuerbacher B and Möhlmann D 1994 *Phys. Rev. Lett.* **73** 652
[53] Hayashi H and Tachibana K 1994 *Japan. J. Appl. Phys.* **33** 804
[54] Melzer A, Trottenberg T and Piel A 1994 *Phys. Lett.* A **191** 301
[55] Kittel C 1956 *Introduction to Solid State Physics* (New York: Wiley) ch 11
[56] Shukla P K and Rosenberg M 1999 *Phys. Plasmas* **6** 1038
[57] Farokhi B, Shukla P K, Tsintsadze N L and Tskhakaya D D 2000 *Phys. Plasmas* **7** 814
[58] Bharuthram R and Shukla P K 1992a *Planet. Space Sci.* **40** 973
[59] Popel S I and Yu M Y 1995 *Contrib. Plasma Phys.* **35** 103
[60] Mamun A A and Shukla P K 2002a *Phys. Plasmas* **9** 1468
[61] Mamun A A and Shukla P K 2002b *Phys. Scr.* T **98** 107
[62] Popel S I, Yu M Y and Tsytovich V N 1996 *Phys. Plasmas* **3** 4313
[63] Popel S I, Gisko A A, Golub A P, Bingham R and Shukla P K 2000 *Phys. Plasmas* **3** 4313
[64] Popel S I, Golub A P and Losseva T V 2001 *JETP Lett.* **7** 396
[65] Shukla P K and Mamun A A 2001 *IEEE Trans. Plasma Sci.* **29** 221
[66] Mamun A A and Shukla P K 2002c *IEEE Trans. Plasma Sci.* **30** 720
[67] Mamun A A, Cairns R A and Shukla P K 1996a *Phys. Plasmas* **3** 702
[68] Mamun A A, Cairns R A and Shukla P K 1996b *Phys. Plasmas* **3** 2610
[69] Mamun A A 1998 *Phys. Scr.* **57** 258
[70] Mamun A A 1999 *Astrophys. Space Sci.* **268** 443

[71] Ma J X and Liu J 1997 *Phys. Plasmas* **4** 253
[72] Singh S V and Rao N N 1997 *Phys. Lett.* A **235** 164
[73] Mendoza-Briceño C A, Russel S M and Mamun A A 2000 *Planet. Space Sci.* **48** 599
[74] Mamun A A and Shukla P K 2001 *Phys. Lett.* A **290** 173
[75] Ivlev A V and Morfill G 2001 *Phys. Rev.* E **63** 0226412
[76] Gupta M R, Sarkar S, Ghosh S, Debnath M and Khan M 2001 *Phys. Rev.* E **63** 046406
[77] Melandsø F and Shukla P K 1995 *Planet. Space Sci.* **43** 635
[78] Shukla P K 2000 *Phys. Plasmas* **7** 1044
[79] Mamun A A, Shukla P K and Verheest F 2002 *Dust Plasma Interaction in Space* ed P K Shukla (New York: Nova) pp 204–55
[80] Bharuthram R and Shukla P K 1992b *Planet. Space Sci.* **40** 647
[81] Vranješ J, Petrović D and Shukla P K 2001 *Phys. Lett.* A **278** 231
[82] Pokhotelov O A, Onishchenko O G, Shukla P K and Stenflo L 1999 *J. Geophys. Res.* **104** 19797
[83] Nakamura Y and Sharma A 2001 *Phys. Plasmas* **8** 3921
[84] Nakamura Y, Bailung H and Shukla P K 1999 *Phys. Plasmas* **9** 440
[85] Luo Q Z, D'Angelo N and Merlino R L 1999 *Phys. Plasmas* **6** 3455
[86] Nakamura Y 2002 *Phys. Rev. Lett.* **83** 1602
[87] Samsonov D, Ivlev A V, Quinn R A, Morfill G and Zhdanov S 2002 *Phys. Rev. Lett.* **88** 095004
[88] Rao N N and Shukla P K 1994 *J. Plasma Phys.* **49** 375
[89] Bernstein I B, Greene J B and Kruskal M D 1957 *Phys. Rev.* **108** 546
[90] Sagdeev R Z 1966 *Reviews of Plasma Physics* vol 4, ed M A Leontovich (New York: Consultants Bureau) p 23
[91] Lonngren K E 1983 *Plasma Phys.* **25** 943
[92] Washimi H and Taniuti T 1966 *Phys. Rev. Lett.* **17** 996
[93] Maxon S and Viecelli J 1974 *Phys. Rev. Lett.* **32** 4
[94] Schamel H 1972 *Plasma Phys.* **14** 905
[95] Schamel H 1975 *J. Plasma Phys.* **13** 129
[96] Schamel H 1986 *Phys. Rep.* **140** 161
[97] Schamel H 2000 *Phys. Plasmas* **7** 4831
[98] Karpman V I 1975 *Nonlinear Waves in Dispersive Media* (Oxford: Pergamon)
[99] Luo Q Z, D'Angelo N and Merlino R L 2000 *Phys. Plasmas* **7** 2370
[100] Hasegawa A 1975 *Plasma Instabilities and Nonlinear Effects* (Berlin: Springer)
[101] Hasegawa A and Mima K 1978 *Phys. Fluids* **21** 87
[102] Hasegawa A 1985 *Adv. Phys.* **34** 1
[103] Larichev V D and Reznik G M 1976 *Dokl. Akad. Nauk. USSR* **231** 1077
[104] Liu J and Horton W 1986 *J. Plasma Phys.* **36** 1